

The Institute of Paper Chemistry

Appleton, Wisconsin

Doctor's Dissertation

The Distribution of the Constituents Across
the Wall of Unbleached Spruce Sulfite Fibers

Otto Kallmes

June, 1959

THE DISTRIBUTION OF THE CONSTITUENTS ACROSS
THE WALL OF UNBLEACHED SPRUCE SULFITE FIBERS

A thesis submitted by

Otto Kallmes

B.S. 1954, Northeastern University
M.S. 1956, Lawrence College

in partial fulfillment of the requirements
of The Institute of Paper Chemistry
for the degree of Doctor of Philosophy
from Lawrence College,
Appleton, Wisconsin

June, 1959

TABLE OF CONTENTS

INTRODUCTION AND PRESENTATION OF PROBLEM	1
SUMMARY OF EXPERIMENTAL RESULTS	4
PRESENT CONCEPT OF FIBER STRUCTURE	5
Structure of Spruce Fibers	6
Primary Wall	8
Secondary Wall	11
Outer Secondary Wall	11
Middle Secondary Wall	12
Inner Secondary Wall	15
Middle Lamella	15
Pit Structure	16
EXPERIMENTAL	17
Isolation of Portion of \underline{P} and \underline{S}_1	17
Preparation of Reclassified Fibers	17
Unravelling of a Portion of \underline{P} and \underline{S}_1	18
Separation of \underline{P} and \underline{S}_1 Fragments from 15,000-count Fibers and Yield Obtained	22
Evidence that Isolated Material is from \underline{P} and \underline{S}_1	23
Unravelling of Middle Secondary Wall	25
Unravelling of \underline{S}_2 in Layers	26
Unravelling of \underline{S}_2 in Sections	30
Examination of Unravelled \underline{P} , \underline{S}_1 , and \underline{S}_2 Material with Light Microscopes	32
Metallurgical Microscope	32
Polarizing Microscope	34
Phase Contrast Microscope	37

Other Microscopes	38
Estimation of Mass of Fibers in \underline{P} and \underline{S}_1	39
Chemical Analyses	40
Hydrolysis	40
Sugar Analysis	41
Alpha-Cellulose and Hemicellulose Determination	43
Degree of Polymerization	45
Degree of Crystallinity	47
Importance of Unravalled \underline{P} and \underline{S}_1 Fragments to Sheet Strength Properties	50
Swelling of Fibers	55
CONCLUSIONS	62
ACKNOWLEDGMENT	65
LITERATURE CITED	66
APPENDIX I. PREPARATION OF PULP	70
APPENDIX II. THEORY OF THICKNESS MEASUREMENTS MADE WITH POLARIZING MICROSCOPE	71
APPENDIX III. DETERMINATION OF INDICES OF REFRACTION BY LINE OF BECKE METHOD	73
APPENDIX IV. SUGAR ANALYSIS	74
APPENDIX V. ORIGINAL DATA	76
F.P.L. Lignin	76
Sugar Analysis	76
Degree of Polymerization	77
Alpha-Cellulose and Hemicellulose Data	77

INTRODUCTION AND PRESENTATION OF PROBLEM

The characteristics of fibers* depend not only on their composition and on the over-all physical properties of the constituents, but to a great extent on the spatial distribution of the constituents within the fiber wall. For example, the strength properties of a sheet of paper are a function of the strength of the bonds between the surfaces of the contiguous fibers. The strength of these bonds is determined chiefly by the composition and the physical characteristics of the outer portions of the fibers. Thus, a knowledge of the constitution and properties of the outer layers is essential to an understanding of the nature of interfiber bonding.

Only a few studies have been made of the distribution of lignin across the fiber wall, and as far as it is known to this author, only two studies have been made of the distribution of the carbohydrates in the fiber wall. The lack of fiber-wall distribution studies is primarily due to the difficulties involved in working with materials with the small dimensions and the small mass (10^{-6} to 10^{-7} g.) (1-2) of individual fibers.

There are three general avenues of approach to distribution studies: (1) The distribution of the constituents within the fiber wall can be hypothesized by deductive reasoning from the behavior of fibers in controlled experiments. This approach, which was taken by Jayme and von Köppen (3), involves considerable speculation. (2) The

* The term fiber as used throughout this thesis refers to untreated as well as delignified longitudinal coniferous tracheids.

distribution of the constituents can be studied in situ by physical methods. This approach was taken by Lange (4) who studied the distribution of lignin and the carbohydrates in the wall of untreated as well as delignified spruce fibers by microspectrographic techniques. The main shortcoming of Lang's techniques is that they give qualitative results. (3) The distribution of the constituents within the fiber wall can be approximated by isolating specific portions of the wall of many fibers and analyzing the isolated materials by chemical techniques. This approach has been applied successfully in the present investigation. Clark (5) also used it in an attempted isolation of the "skin substance" (the primary wall) of bleached sulfite fibers. He did not analyze the isolated material, apparently because he failed to identify positively its origin in the fiber wall. Clark's isolation was carried out by a procedure which is similar to the one developed in this investigation.

It has been known for a long time that fibers consist of four concentric walls, and that these walls are bonded relatively loosely to each other (6). Therefore, it was believed at the outset of this investigation that it should be possible to unravel and isolate in identifiable form specific walls of the fiber. Early in the experimental program it was discovered that the two outer walls unravel simultaneously. These two walls together constitute a small fraction of the fiber mass. With this limitation in mind, the following specific objectives were set for this thesis:

(1) To isolate portions of the primary and outer secondary walls (P and S₁) and of the middle secondary wall (S₂) of unbleached spruce sulfite fibers in a definable form. The quantities isolated should represent a significant proportion of the amounts present in the fibers.

(2) To establish positively by microscopic comparisons the origin of the isolated materials in the fiber wall.

(3) To study the structural details and chemistry of the isolated materials.

SUMMARY OF EXPERIMENTAL RESULTS

A technique has been developed for isolating P-S₁ material and S₂ material from delignified fibers in sufficiently large quantities for chemical analyses. From the analyses of the P-S₁ and S₂ materials and the original fibers, it was possible for the first time to approximate the distribution of the constituents across the wall of unbleached spruce sulfite fibers. These distributions are as follows:

The concentration of lignin in P and S₁ is 10 to 20 times as large as in S₂ (Ca 5.8 versus 0.4%). The concentrations of alpha-cellulose (81.3%) and the hemicelluloses (12.9%) in P and S₁ are slightly lower than in S₂ (82.6-84.0% and 17.0-15.5% respectively). The hemicellulose distribution is consistent with the distribution of the sugars, glucose, mannose, and xylose, which are present in an essentially constant ratio (29:2:1) across the fiber wall. The D.P. of P and S₁, 2030, is about two thirds of that of S₂. P and S₁ are partly crystalline, but not as much as S₂.

Two related experiments were carried out. (1) It was found that unravelled P and S₁ fragments can enhance sheet strength properties considerably. (2) Two theories of Wardrop and Dadswell (56) on balloon-type swelling were corroborated. These theories are that S₁ is primarily responsible for the constrictions observed during ballooning and that the "skin substance" concept is unnecessary to explain ballooning.

PRESENT CONCEPT OF FIBER STRUCTURE

Spruce fibers are elongated four-to-six sided cells which, in the native wood, average 3.3 mm. in length and 25 to 30 μ in tangential width (7). Their radial width varies from 25 to 30 μ in early springwood fibers to 5 to 10 μ in late summerwood fibers. The main constituents of the fiber wall are cellulose, the hemicelluloses, and lignin.

Cellulose is a linear polysaccharide made up of D-glucose anhydride units linked through 1-4 β -D-glycosidic bonds. In sprucewood, the cellulose chains each contain 7000 to 10,000 units (8) and they are arranged parallel to one another in more and less crystalline states within microfibrils; microfibrils are structural units 150-250 A. in diameter and of indefinite length (9-10). Discussions of the arrangements of the microfibrils within the fiber wall are presented in the following sections.

The degree of crystallinity of the cellulose within the microfibrils varies in a regular manner (2). About 70% of the cellulose of untreated spruce fibers is present in dense, highly crystalline regions which give a sharp x-ray pattern (2). These regions are known as micelles; they are 50-100 A. wide, less than 50 A. thick, and 500-600 A. long (9, 11, 12). The micelles are embedded in less crystalline cellulose known as paracrystalline or amorphous cellulose which gives a diffuse x-ray pattern. The internal structure of microfibrils according to Frey-Wyssling (9) is shown in Figure 1a. (The lines of this figure indicate the orientation of the individual cellulose chains.)

The hemicelluloses are linear as well as partially branched noncellulosic polysaccharides. They differ from the cellulose in their shorter chain length, and in that they can be extracted readily from delignified fibers by alkali. They do not constitute a definite proportion of the fiber but are defined on the basis of their preparation, such as the hemicelluloses soluble in 17.5% sodium hydroxide. These hemicelluloses constitute about one fourth of the carbohydrates of spruce-wood and are composed of units of glucose, mannose, galactose, arabinose, xylose, and of uronic anhydride units.

Lignin is present between the microfibrils although there is some evidence that it penetrates the paracrystalline regions to a small extent (2). Because the lignin cannot be extracted entirely from fibers without removing a portion of the hemicelluloses, some investigators (2-3) believe that the two are chemically bound. However, the existence of such a bond has not yet been fully demonstrated. Lignin constitutes about 28% of the weight of sprucewood and 0.5-5% of spruce sulfite fibers. It is aromatic in nature, but its structural details are only partially known.

STRUCTURE OF SPRUCE FIBERS

On an ontogenetic basis, fibers consist of two concentric walls, the tenuous P , and the relatively thick secondary wall (see Figure 1b). On the basis of microfibrillar orientation, the secondary wall of normal fibers can generally be subdivided into three concentric walls, the thin S_1 and S_3 , and S_2 whose thickness varies from fiber to fiber.

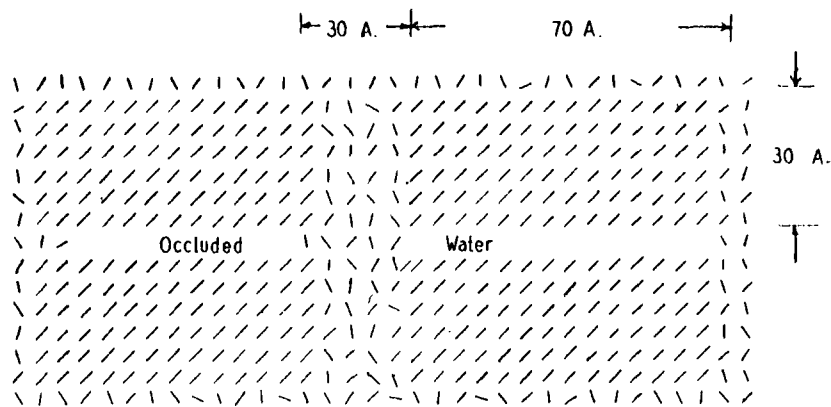


FIGURE 1A
Cross section of Microfibril Showing Four Micelles
Embedded in Paracrystalline Cellulose (9)

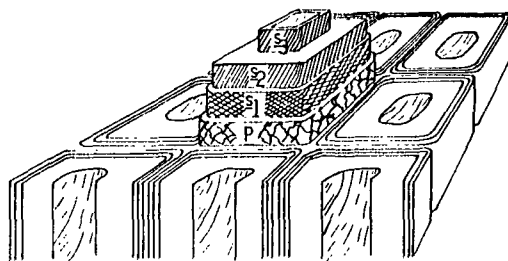


FIGURE 1B
Wall Structure of Spruce Fibers. (2)

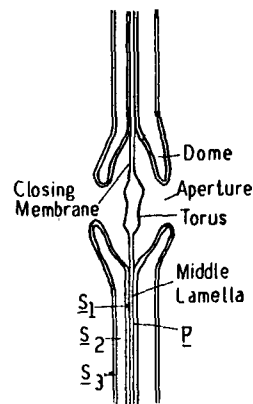


FIGURE 1E
Pit Structure. (2)

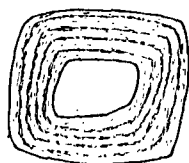


FIGURE 1C
S₂ with Concentric Layering (16)

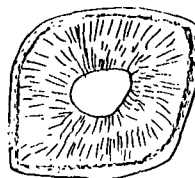


FIGURE 1D
S₂ with Radioconcentric Layering (16)

The lateral bonds between \underline{P} and \underline{S}_1 , between \underline{S}_1 and \underline{S}_2 , and between the various layers of \underline{S}_2 of delignified fibers are relatively weak (6, 15). The weakness of these bonds makes it possible to unravel consecutively the various fiber walls by a light mechanical action.

Primary Wall, P

The primary wall is a thin, loosely woven network of microfibrils which, in untreated fibers, are embedded in a matrix of lignin and hemicelluloses (13). The thickness of \underline{P} is believed to be nonuniform (16); values of 0.1-1 μ have been reported for its average thickness (17). It is well-known from electron microscope studies that the microfibrils of \underline{P} are interwoven and that they are more or less randomly oriented in a generally transverse direction to the longitudinal fiber axis (9, 13, 18, 19).

I. W. Bailey (16) has shown that "the grosser visible texture of the primary wall is due to inequalities in thickness which produce a variety of banded, striated, reticulated, and other structural details....When the tenuous \underline{P} walls are freed from their noncellulosic constituents, they persist as an extremely porous, but firmly coherent matrix of anisotropic cellulose, the finer thread-like structural details of which grade down to the limits of microscopic visibility....The thicker parts of the primary wall, when carefully swollen, exhibit a distinct lamination." Some of the structural details of \underline{P} are shown in Figures 2-5. The fibrillar network of Figure 2 is similar to Figure 4 of reference (16).

Few data are available on the chemical composition of P. Numerous investigators (15, 20, 21, 22) have shown that in conifers, the concentration of lignin in P is higher than in the secondary wall. Lange (23, 24) estimated that P of untreated Swedish spruce fibers contained 60 to 90% lignin, and that 60% of the carbohydrates are hemicellulosic and 40% cellulosic.

Giertz and Nisser (25), using a staining technique, estimated that less than 14% of P is removed during the preparation of a strong or medium strong sulfite pulp; a medium strong pulp was used in this study.

Jayme and von K^uppen (3) investigated the differences between unbleached spruce sulfite and sulfate pulps each with the same Halse lignin content, 3.6%. The differences between the pulps were attributed in part to different distributions of the constituents across the fiber walls, and in part to differences in the composition of P and S₁. It was found that in the sulfite pulp, the concentration of lignin in P and S₁ was about 10 times that in S₂; in the sulfate pulp, the lignin was distributed uniformly across the fiber wall. Jayme and von K^uppen assumed that the hemicellulose distribution followed the lignin distribution in both pulps. They indicated that the D.P. of the carbohydrates increased from about 300 at P to about 2000 at the lumen in the sulfite pulp, and in a similar manner from 1000 to 1500 in the sulfate pulp. It was not shown how these D.P. distributions were calculated. These investigators concluded that the sulfite pulp beat faster and swelled more because of the higher hemicellulose content and lower D.P.



Figure 2
Reclassified Fiber and
Attached P Fragment
(M*, 440X)



Figure 3
Reclassified Fibers and
Attached P Fragments
(M, 84X)



Figure 4
Enlargement of Figure 3
(M, 440X)

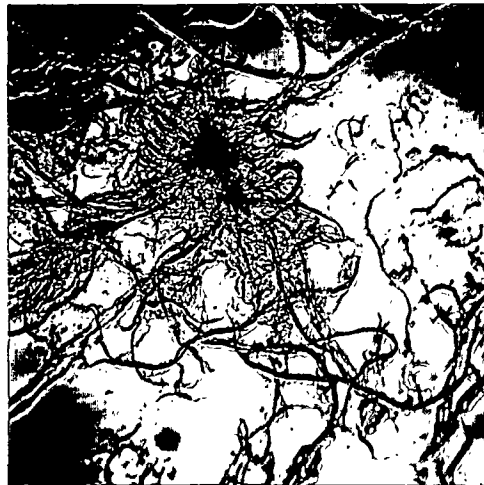


Figure 5
Isolated P Fragment
(M, 440X)

* Microphotograph taken with metallurgical microscope

of its \underline{P} and \underline{S}_1 . The lower strength properties of the sulfite pulp were attributed to the relatively weak interfiber bonds formed by the hemicelluloses and the short-chained cellulose, and to the high concentration of lignin in \underline{P} and \underline{S}_1 . It was believed that the lignin in \underline{P} and \underline{S}_1 reduced the amount of interfiber bonding.

(In the present investigation, it was demonstrated that the assumed hemicellulose and the indicated D.P. distributions of the sulfite pulp were incorrect.)

Secondary Wall

The microfibrils of each of the three secondary walls are oriented parallel to one another and they are more densely packed than in \underline{P} . The main differences among the three walls exist in the orientation of their microfibrils with respect to the longitudinal fiber axis. The microfibrils of \underline{S}_2 are oriented more or less parallel to the fiber axis while in most species the microfibrils of \underline{S}_1 and \underline{S}_3 are oriented more or less perpendicular to it. In a few species, including spruce, the microfibrils in \underline{S}_3 are oriented similarly to those in \underline{S}_2 .

Outer Secondary Wall, \underline{S}_1

It has long been known that \underline{S}_1 is a thin membrane and that its microfibrils are oriented parallel to each other and in a more or less transverse direction to the longitudinal fiber axis (26). Recently James and Wardrop (27) found that on lightly beating certain pine pulps, membranous fragments containing two crossed sets of parallel fibrils were unravelled

from the fibers. Emerton and Goldsmith (6) have since demonstrated that these fragments originated from S_1 , and this finding has been confirmed for spruce by Meier (28). Emerton (29) also showed that S_1 is probably less than $.5 \mu$ thick, that the two sets of fibrils spiral in opposite senses to the longitudinal fiber axis, and that the angle between a tangent to either set of fibrils and the longitudinal fiber axis (hereafter referred to as the fibrillar angle) is about 60° . It has also been shown by other investigators (28, 30) that both sets of fibrils are not invariably present in the unravelled S_1 fragments; one set appears to be missing over some areas for unknown reasons. It should be pointed out that these findings were made mainly with light microscopes and that the observed fibrils are not identical with the microfibrils. The fibrils are believed to be bundles of microfibrils aggregated like the micelles in microfibrils (6, 30, 31).

Numerous other structural details for S_1 have been proposed (6, 28, 30). They are not discussed here because little is definitely known about them. There is only sparse information available on the relative quantities of the constituents present in S_1 . On the basis of micro-spectrographic evidence, Lange (23) proposed that in untreated spruce fibers the concentration of lignin across S_1 increases from about 20% at its S_2 border to about 60% at its P border. He also estimated that the cellulose to hemicellulose ratio is about the same as in P .

Middle Secondary Wall, S_2

The S_2 contains the bulk of the fiber mass. In each growth ring

of sprucewood, the thickness of S_2 gradually increases from about one micron in the early springwood fibers to over five microns in the late summerwood fibers (31). The S_2 of untreated spruce fibers contains 75-90% carbohydrates and 25-10% lignin in two continuous, interpenetrating systems, either of which can be dissolved out without seriously modifying the structure of the remaining one (16, 23).

According to Bailey (16), the carbohydrates and lignin are not distributed uniformly throughout S_2 of untreated spruce fibers, but are grossly divided into carbohydrate- and lignin-rich layers which form two different patterns, concentric and radioconcentric. Both patterns are widespread, and in some cases both are present within a single fiber. The carbohydrate and lignin-rich layers also vary greatly in their radial dimensions and in their texture. A fine texture refers to the case where individual microfibrils or bundles of a few microfibrils are embedded in the lignin matrix, and to where the interfibrillar pores occupied by the lignin are fine; a coarse texture refers to fibrils embedded in the lignin, and to large interfibrillar pores.

The concentric and radioconcentric patterns of S_2 are illustrated in Figures 1c and 1d. The concentric layering, which may consist of as many as 35 cellulose-rich layers in spruce summerwood fibers (32), has been observed by numerous investigators (13, 33-35). Besides Bailey (16), only Wardrop and Dadswell (36) have reported radioconcentric layering of S_2 ; they found it in the compression wood of certain pines.

Upon delignification, the originally lignin-rich layers become planes of weakness (16, 37). Therefore, fibers whose S_2 has a concentric layering may undergo considerable fibrillation in layers during mechanical treatment (33). However, no references were found concerning the fibrillation of fibers whose S_2 had a radioconcentric layering.

The cellulose of S_2 forms microfibrils which are oriented parallel to each other and which, in spruce, almost invariably spiral around the longitudinal fiber axis with a Z-form (1); i.e., the microfibrils appear to turn clockwise as they recede from an observer looking down the longitudinal fiber axis. The fibrillar angle varies from 0 to 50°, and some evidence (38) has been found that the size of this angle decreases with increasing fiber length.

Few data are available on the over-all distribution of the lignin and the carbohydrates within S_2 . Lange (39) found that lignin comprises 10-20% of the mass at the lumen of untreated spruce fiber, and that it increases only slightly across S_2 . He also found that the carbohydrates are distributed more or less uniformly across S_2 . However, the cellulose which constitutes about 85% of the carbohydrates at the lumen decreases linearly to about 40% at the S_1 border. The hemicelluloses, on the other hand, constitute 15% of the carbohydrates at the lumen and about 60% at the S_1 border.

No data are available on the distribution of cellulose and hemicelluloses in S_2 of unbleached spruce sulfite fibers. Jayme and von Köppen (3) have shown that the lignin is distributed more or less uniformly across

S₂ of these fibers, and Asunmaa and Lange (40) have shown that the density of the carbohydrates decreases linearly from the lumen to the S₁ border. They attribute this carbohydrate-density distribution to a preferential removal during cooking of a portion of the hemicelluloses from the outer layers of S₂.

Inner Secondary Wall, S₃

The S₃ of most species is similar to S₁ in its dimensions and microfibrillar orientation (1). A layer similar to S₁ is not present on the inner surface of S₂ of normal spruce fibers and, therefore, Wardrop and Dadswell (35) concluded that S₃ is absent from this species. On the other hand, considerable evidence of a thin but unique layer inside S₂ of spruce fibers has been obtained by Bucher (41) using specific dyes, and by Meier (19) and Asunmaa (42) using wood-rotting fungi. These investigators have shown that the innermost layer of the spruce fiber wall, which they refer to as the tertiary wall rather than S₃, has a fibrillar orientation similar to that of S₂. Meier and Yllner (43) have also shown that S₃ of spruce is well preserved in holocellulose, but badly damaged in bleached sulfite fibers.

Middle Lamella

In the wood, the fibers are embedded in an isotropic amorphous matrix known as the middle lamella. Between contiguous fibers, this layer is 0.2-0.5 μ thick (19), and it is composed mainly of lignin and of small quantities of what may be hemicellulosic and/or pectic materials (2, 44).

It is removed entirely during sulfite cooks that leave a lignin content in fibers as low as the one obtained in the present investigation (15).

Pit Structure

In the cambial zone of living trees, the protoplasm of contiguous cells is connected at intervals along their radial walls. When the cells mature, pits, which are breaks in the normal structure of S_2 , form at these intercellular connections. Rows of pits at 10-20 μ intervals are visible on the radial surfaces on many springwood fibers; they are not readily visible on the thicker-walled summerwood fibers.

The cross-sectional view of a typical pit is shown in Figure 1e. The pit opening, the aperture, is surrounded by a band of circularly oriented cellulose, called the dome, which is a portion of the secondary wall. The dome is lined on its inner and outer surfaces by S_3 and S_1 (21, 41).

The closing membrane separates the adjacent pits, and in the sapwood acts as a valve to the flow of liquids. The thickening in the center of the closing membrane is called the torus; the torus is impermeable to the flow of liquids and its fibrils are circularly oriented (45, 46). The microfibrils of the remainder of the closing membrane, on which the torus is suspended, are radially oriented in a spoke-like manner.

EXPERIMENTAL

ISOLATION OF A PORTION OF P AND S₁

PREPARATION OF RECLASSIFIED FIBERS

The isolation of a portion of P and S₁ was based on the size difference between unravelled P and S₁ fragments and the parent fibers. Therefore, ray cells and miscellaneous pulping debris, which were approximately the same size as P and S₁ fragments, had to be separated from the fibers in order to obtain an uncontaminated product. The preparation of debris-free fibers was carried out by the following procedure.

Chips of white spruce [Picea glauca (Moench) Voss], carefully screened from sawdust and knots, were pulped by a long, low temperature calcium-base sulfite cook. The initial composition of the cooking liquor was as follows: total SO₂ = 7.27%, free SO₂ = 6.09%, and combined SO₂ = 1.18%. The maximum temperature was 131°C. and the total cooking cycle 13 hours. Details of the cook are given in Appendix I.

The chips were cooked in a removable basket mounted in the digester in order to eliminate fiber damage that might have been incurred by blowing the digester. The pulp was washed for five ten-minute periods with warm deionized water under gentle agitation. The washed pulp was only partially defiberized, and the residual chips were broken up by hand into individual fibers and small fiber bundles. The fiberized pulp was screened by a flat screen with 0.010-inch openings; the screening rejects were discarded.

The screened pulp was classified in ten-gram batches for six minutes in the first two compartments of the Bauer-McNett classifier fitted with the 8- and 12-mesh screens. Only the fibers retained by the classifier were treated further; the filtrate from the 12-mesh screen was discarded.

The remaining fiber bundles of the once-classified pulp were broken up in a 20-minute treatment (2500 counts) in a British disintegrator. (The propeller of the disintegrator has a speed of 7500 counts/hour; 1 count = 25 rev.) A consistency of 1% was used in this and in all subsequent disintegrator treatments. Because a small quantity of ray cells was freed during the breaking up of the fiber bundles, the pulp was classified again under the conditions outlined above. The fibers retained by the classifier at the end of the second classification were equal to less than 10% of the screened pulp, and hereafter they are referred to as reclassified fibers. A microscopic examination of the reclassified fibers revealed that they were almost completely free of ray cells, cut fibers, and debris.

UNRAVELLING OF A PORTION OF \underline{P} AND \underline{S}_1

The walls of the reclassified fibers were unravelled consecutively and randomly from all fiber surfaces by prolonged stirring in the British disintegrator. In the first 12,500 counts (i.e., after a total of 15,000 counts) only \underline{P} and \underline{S}_1 were unravelled. The material unravelled thereafter became increasingly poor in \underline{P} and \underline{S}_1 material and increasingly rich in \underline{S}_2 material. Unravelling of \underline{S}_2 is discussed in detail later.

The outermost wall, P, of mechanically undamaged fibers had to unravel first. A small amount of material believed to originate from P was partially unravelled during the preparation of the reclassified fibers; i.e., it was unravelled but remained attached to the fibers (See Figures 2-4). The fragment in Figure 2 is believed to be a membranous P fragment for four reasons: (1) It has a sieve-like structure. (2) It is similar in appearance to P fragments obtained by I. W. Bailey (16). (3) It was among the first material unravelled from the fibers. (4) Its membranous nature is evident from the interference fringes parallel to the lower edge of the bright area below the fiber. Emerton (47) has shown that as a fiber goes through the last stages of drying, it shrinks and draws taut membranes which are attached to it and which are also bonded to the substrate. When the wedge-shaped air gap between the membrane and the substrate is illuminated with vertically reflected light, an interference pattern similar to Newton's rings is formed.

The material attached to the fiber in Figure 3, of which a portion is shown enlarged in Figure 4, is typical of most of the first material unravelled from the fibers. It includes fragments which appear to be membranes composed of randomly oriented fibrils and some individual fibrils. It cannot be proven that these fragments are truly membranous P fragments and that they are not flocculated fibrils. However, these fragments, or their constituent fibrils, originated from P or S₁ for two reasons. (1) Unravelled S₂ material has an entirely different structure. (2) S₂ material is not unravelled until the fibers have been stirred over 15,000 counts.

Figure 5 shows a completely unravelled fragment similar to those in Figure 4. If the fragment in Figure 5 is truly membranous, it originated from P because its fibrils are randomly oriented. If it consists of flocculated fibrils, it is likely that the fibrils originated primarily from P for the following reason. During the early stages of stirring (before 15,000 counts), the fraction of P unravelled had to be equal to or greater than the fraction of S₁ unravelled. Fragments like the one in Figure 5 unravelled in more or less equal quantities with identifiable S₁ fragments after 3500 counts. Therefore, fragments similar to the one in Figure 5 are referred to as P fragments hereafter.

Individual fibrils indistinguishable from those in Figure 3-5 were unravelled along with S₂ material during the later stages of stirring. There are no reasons to believe that individual fibrils were removed preferentially from S₂ before the bulk of this wall was unravelled. It is therefore concluded that the individual fibrils unravelled during the first 15,000 counts originated primarily from P and S₁.

In the stirring interval between 3500 and 15,000 counts, a large quantity of P and S₁ fragments was unravelled. Typical S₁ fragments are shown in Figures 5-11; they are similar in appearance to S₁ fragments obtained by Emerton and Goldsmith (6) and by Wardrop (30). The S₁ fragment in Figure 6 appears to have unravelled from the adjacent fiber because it contains pit impressions in mirrored-image positions of pits on the fiber. To an observer looking down the longitudinal fiber axis from the right of Figure 6, the S₁ fragment unravelled in a clockwise direction,

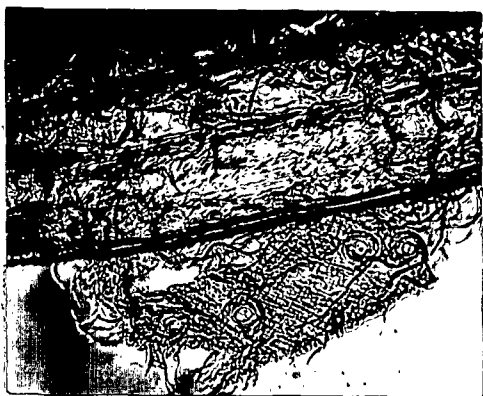


Figure 6
15,000-count Fiber and
Attached S_1 Fragment (M, 440X)



Figure 7
15,000-count Fiber and Attached
 S_1 Fragments (M, 440X)

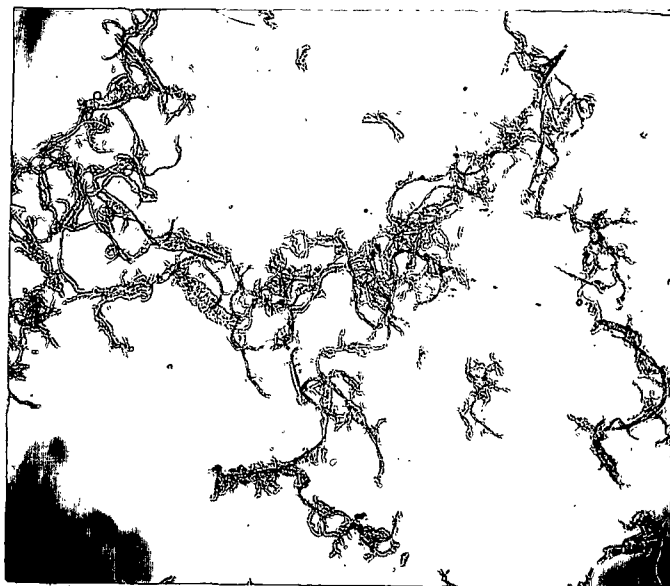


Figure 8
Isolated P and S_1 Fragments (M, 84X)

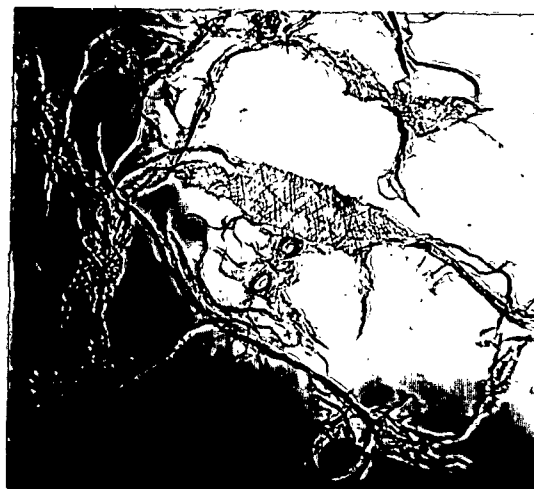


Figure 9
Isolated S_1 Fragments, Enlarged
from Figure 8 (M, 440X)



Figure 10
Isolated S_1 Fragment (M, 440X)



Figure 11
Isolated S_1 Fragment (M, 440X)

i.e., from beneath the fiber. The two sets of fibrils of the fragments in Figures 6, 7, 10, and 11 all have an obtuse and approximately equal fibrillar angle.

Relatively few S_1 fragments were found in which one set of fibrils was partially absent. Therefore, it is concluded that S_1 of Picea glauca contains, for the most part, two sets of fibrils which have the same fibrillar angles.

SEPARATION OF P AND S_1 FRAGMENTS FROM 15,000-COUNT FIBERS AND YIELD OBTAINED

The P and S_1 fragments were separated from the 15,000-count fibers in the Bauer-McNett classifier run on deionized water. Only the first compartment of the classifier, fitted with the 200-mesh screen, was used. Three-gram batches of 15,000-count fibers were classified for four minutes. The P and S_1 fragments were in the filtrate which was collected; the fibers were retained by the classifier.

The concentration of P and S_1 fragments in the classifier filtrate was less than 0.1 g./l. The fragments were flocculated by centrifuging the filtrate for 15-minute periods in an International centrifuge (size 1, type SB) run at 1800 r.p.m. The water above the flocculated particles was siphoned off, and the flocs from several centrifuge bottles were combined and centrifuged again. Repeating this procedure numerous times gradually built up the concentration of fragments to several hundred milligrams per 50 ml. About one week was required to concentrate the P - S_1 material from three grams of 15,000-count fibers.

The isolated P-S₁ material hornified when dried directly from water and, therefore, the water was replaced by acetone by the solvent-exchange method. The P-S₁ material was dried from acetone on microscope slides in sheet form under vacuum at room temperature. The sheets, each weighing approximately two milligrams, were peeled off the slides with a razor blade.

For visual inspection, the P and S₁ fragments were dried on microscope slides directly from the classifier filtrate under vacuum at room temperature.

A yield of 3.3% or 0.217 g. of P-S₁ material was obtained from 6.53 g. of 15,000-count fibers. As is shown in a later section (page 39) P and S₁ together comprise between 5 and 20% of the fibers' mass. Therefore, the material isolated represents 15 to 65% of the available P-S₁ material.

EVIDENCE THAT ISOLATED MATERIAL IS FROM P AND S₁

Slides of the isolated P and S₁ fragments were metal-shadowed with chromium by Emerton's technique (6) and examined with a metallurgical microscope. Unshadowed slides were studied with a polarizing and a phase contrast microscope. The following observations were made:

No ray cells were present. Had a few undetected ones been present, their mass contribution to the isolated P-S₁ material would have been negligible because their walls are less than one micron thick.

A negligible quantity of S_2 material was present.

All of the isolated material was birefringent. The lack of isotropic material showed that material from the middle lamella was absent (21).

About one half of the isolated fragments were S_1 fragments and the other half P fragments. Figure 8 is a typical view of a slide of isolated P and S_1 fragments. The structural details of the fragments of this photomicrograph are difficult to distinguish without further magnification and, therefore, two S_1 fragments are shown enlarged in Figure 9. Figure 8 is presented only to demonstrate that the isolated $P-S_1$ material contained no unidentifiable debris. More typical isolated S_1 fragments are shown in Figures 10 and 11.

Portions of pit domes, and occasionally the entire domes, were attached to some S_1 fragments. This was revealed in thickness measurements of S_1 fragments which are discussed later. It was found that the thickness of S_1 , 0.5μ , varied at the domes from about 0.5μ up to about 2μ . It is believed that pit dome material represented a contamination of an indefinite, but certainly very small percentage.

It was not possible to determine the purity of $P-S_1$ material quantitatively. However, after carefully examining many slides, it can be safely concluded that the $P-S_1$ material contained less than 10%, and probably less than 5% contamination.

UNRAVELLING OF MIDDLE SECONDARY WALL

The reclassified fibers were stirred a total of 300,000 counts in the British disintegrator. At 15,000 counts, they were classified to remove the unravelled $P-S_1$ material. At 30,000, 50,000, 75,000, and at 100,000 counts, they were classified in four-gram batches for ten-minute periods in the first compartment of the classifier fitted with the 100-mesh screen. At 128,000, 160,000, 200,000, 250,000, and at 300,000 counts, they were classified in four-gram batches for fifteen-minute periods by the 65-mesh screen. The reason for intermittently removing the unravelled material was to make it possible to follow the gradual breakdown of the fibers without their being cluttered by debris.

In the stirring intervals above 15,000 counts, the quantities of $P-S_1$ material unravelled became smaller and smaller. Above 200,000 count, only trace quantities were removed from the fibers. The presence of only a small fraction of S_1 on a few 300,000-count fibers was confirmed in fiber swelling studies.

The S_2 material was first unravelled in tiny quantities between 15,000 and 20,000 counts and in increasingly large quantities thereafter. Above 50,000 counts, material from S_2 predominated among the unravelled material.

The S_2 disintegrated in two distinctly different ways. Between 20,000 and 50,000 counts, the material removed from S_2 consisted almost entirely of membranous layers. Beginning at 50,000 counts, whole sections

of the \underline{S}_2 walls were literally ripped out of the fibers. The quantities of \underline{S}_2 layers and \underline{S}_2 wall sections removed from the fibers increased steadily with increased stirring time.

UNRAVELLING OF \underline{S}_2 IN LAYERS

Unravelling of \underline{S}_2 in layers is illustrated in Figures 12-14. The membranous nature of the unravelled layers is evident from the interference patterns of Figure 12. The layer shown in this figure unravelled from the top surface of the springwood fiber on the left and draped itself over the summerwood fiber on the right.

Figure 13 shows a partially unravelled layer attached to the fiber at a fold which makes an angle of 45° to the longitudinal fiber axis. The faint white line which runs parallel to the fiber axis and to the left from the lower left-hand corner of the fold indicates where the unravelled layer was torn from its layer of the fiber. A single set of fibrils oriented parallel to each other and to the fiber axis is visible both above and below the tear line. From simple geometric considerations, it can be seen that the single set of parallel fibrils of the unravelled layer was also oriented parallel to the fiber axis prior to its removal from the fiber. Because it has been well-established that only \underline{S}_2 (and the disputed \underline{S}_3) of spruce has this fibrillar orientation, it is concluded that the unravelled layer in Figure 13 originated from \underline{S}_2 .

Further evidence that unravelled layers similar to those in Figures

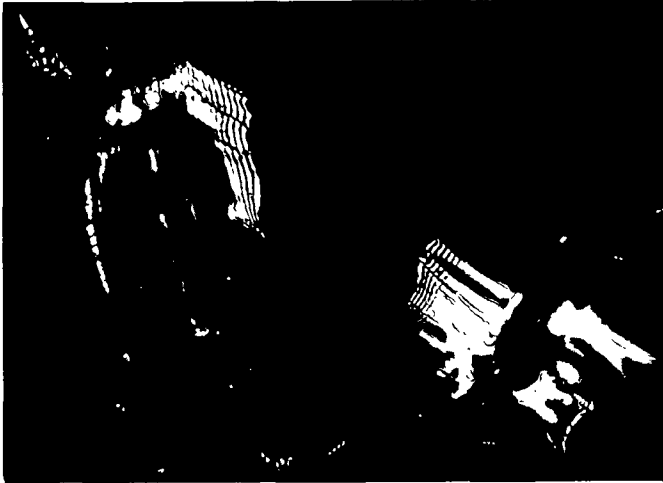


Figure 12
300,000-count Fiber & Attached
 S_2 Layer (M, 440X)

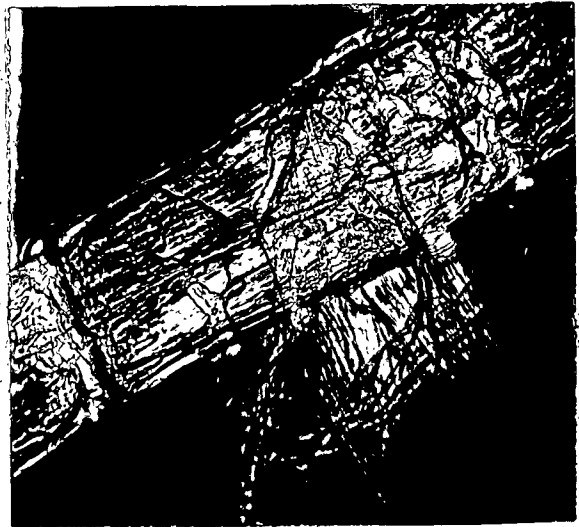


Figure 13
300,000-count Fiber & Attached
 S_2 Layer (M, 440X)

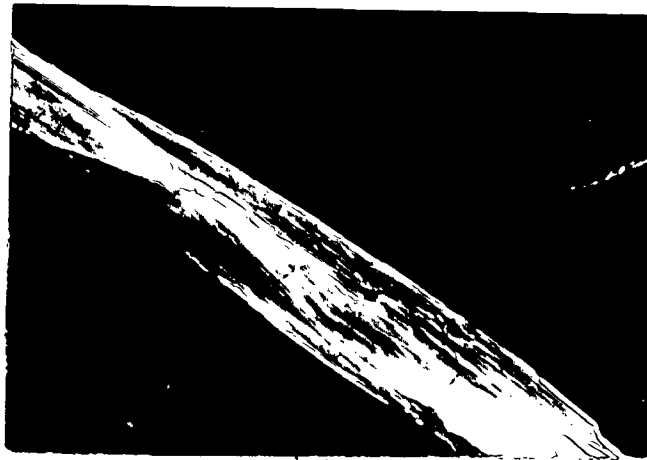


Figure 14
Unravelled S_2 Layers
(P*, 375X)

* Photomicrograph taken with polarizing microscope

12 and 13 contain only a single set of parallel fibrils was obtained in examinations made between crossed nicols. Figure 14 shows two equally thick unravelled layers. The one which is readily visible appears to contain a single set of well-defined parallel fibrils whereas the layer in the upper right-hand corner is almost at extinction. Because layers like those in Figure 14 are almost invisible at the extinction positions, their fibrils must be oriented parallel to each other; therefore, they must have originated from S_2 (or the disputed S_3).

Many fibers similar to those in Figures 15 and 16 were unravelled down to their innermost layers. In Figure 15, the fibrils of S_2 (or S_3) form a broad helix and have the appearance of crossed fibrils. A similar fiber whose top layer has been split open and folded back above the fiber is shown in Figure 16. Here one is looking at the innermost layer of the fiber from the lumen side. The transverse cracks in the upper section were probably caused by shrinking of the fibrils during drying. If one imagines the folded back layer in its original position, the fiber would be identical in appearance to the one in Figure 15. From both Figures 15 and 16 it is evident that the fibrillar angle of the innermost layer of spruce fibers is small and similar to that of the bulk of S_2 . This finding is in agreement with results obtained by Wardrop and Dadswell (35), Meier (19), and Bucher (41).

The unravelled S_2 layers are not basic structural units of fibers (16). It is believed that the lignin-rich layers of the untreated fibers, which become relatively porous during delignification, are planes



Figure 15
300,000-count Fiber
(M, 440X)



Figure 16
300,000-count Springwood Fiber
with Innermost Layer Seen from
Lumen-side
(M, 440X)

of weakness in the delignified fiber wall (33-37) at which the fibers split preferentially during mechanical treatment. The unravelled S₂ layers are not necessarily single cellulose-rich layers, but may be several which split off as a unit.

UNRAVELLING OF S₂ IN SECTIONS

It was found that whole sections were literally ripped out of the S₂ walls of many fibers after 50,000 counts of stirring (Figures 17 and 18). In most cases, the S₂ wall sections were found torn free from the fibers like the one in Figure 20.

The bulk of the S₂ wall sections consisted of fibrils of varying diameters (Figure 19). A few long and numerous short thin S₂ layers were found attached to the wall sections. Their central portion was generally two to three microns thick, and for this reason it is believed that they originated primarily from the summerwood fibers.

The S₂ wall sections differed from P fragments in three ways:

(1) They were not removed from the fibers until after 50,000 counts of stirring. (2) They invariably had numerous thin S₂ layers attached to them; these were missing completely from P fragments. (3) They were much larger than P fragments.

The information obtained in this investigation on S₂ wall sections is of a preliminary nature, and without considerably more evidence, conclusions cannot be drawn. However, it is hypothesized by this author that the formation of wall sections may be explained on the basis of the

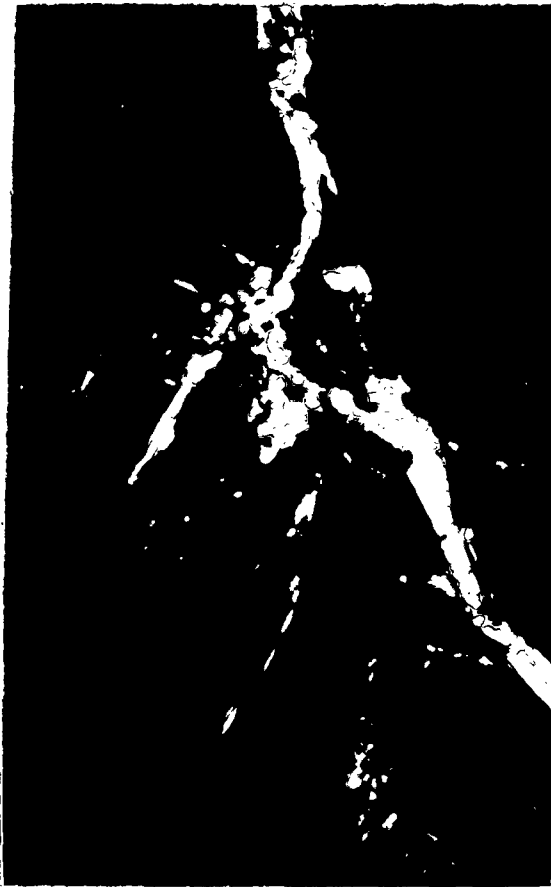


Figure 17
300,000-count Summerwood Fiber and
Attached S_2 Wall Section (P, 190X)

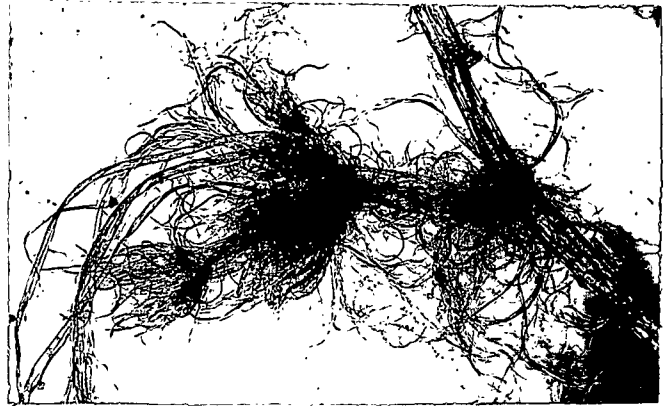


Figure 19
Same as Figure 18 (M, 95X)



Figure 20
Unravalled S_2 Wall
Section (M, 95X)

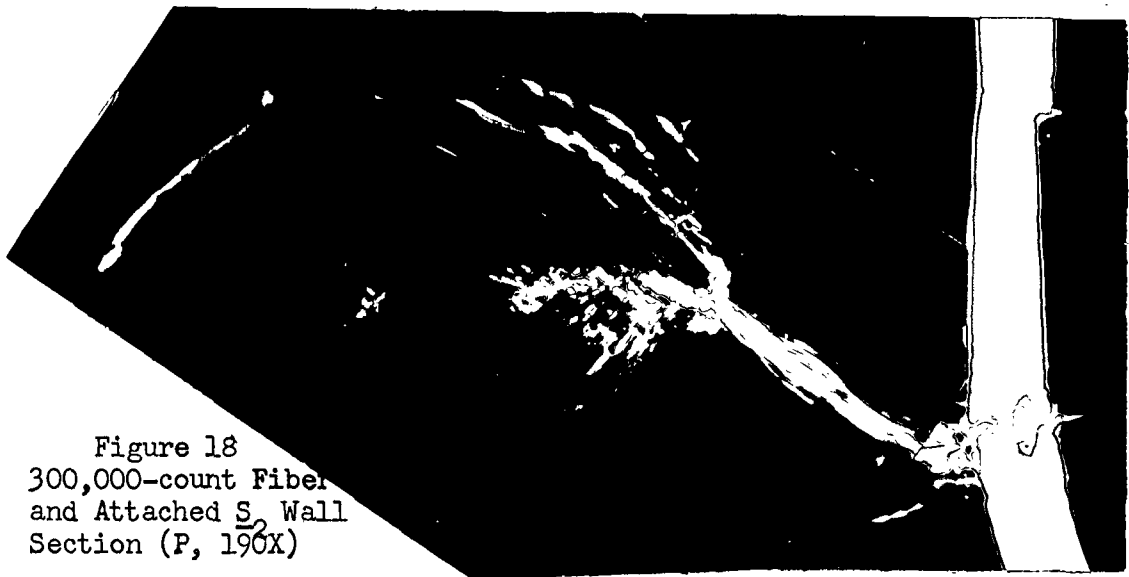


Figure 18
300,000-count Fiber
and Attached S_2 Wall
Section (P, 190X)

radioconcentric layering of \underline{S}_2 proposed by Bailey (16). It is postulated that the wall sections were torn from the fibers primarily at the radial planes of weakness which were formed by the delignification of fibers whose \underline{S}_2 had a radioconcentric layering. It is also suggested that fibers which originally had both types of \underline{S}_2 layering fibrillated in long, thin \underline{S}_2 layers and in wall sections like the fiber in Figure 18.

EXAMINATION OF UNRAVELLED \underline{P} , \underline{S}_1 , AND \underline{S}_2 MATERIAL WITH LIGHT MICROSCOPES

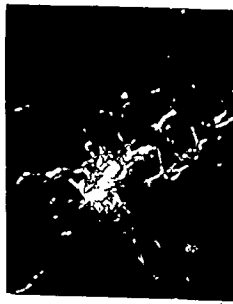
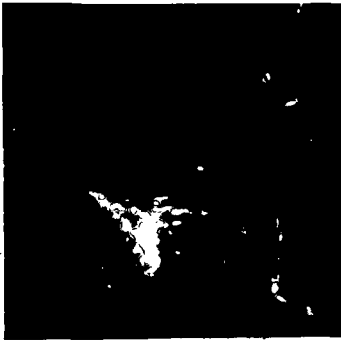
METALLURGICAL MICROSCOPE

The gross structural details of the fibers and the unravelled \underline{P} , \underline{S}_1 , and \underline{S}_2 material were seen most clearly with a metallurgical microscope, especially if the slides were first metal-shadowed (6). Most of the photomicrographs for this investigation were taken with a Bausch and Lomb metallurgical microscope.^a

The only dimension measured on the photomicrographs taken with the metallurgical microscope was the fibrillar angle of \underline{S}_1 fragments. The size of this angle varied somewhat, not only among the \underline{S}_1 fragments, but within individual fragments. It is not known whether this is an intrinsic variation of \underline{S}_1 or whether it was caused during the preparation of the samples. The fibrillar angle, measured in undistorted portions of 14 \underline{S}_1 fragments, was $57.4^\circ \pm 15.5^\circ$ ^b. This angle is in approximate

^a This microscope was made available through the courtesy of Appleton Wire Works, Appleton, Wisconsin

^b 95% Confidence limits.



Figures 21 & 22
Isolated P Fragments (P, 375X)



Figures 23 & 24
Isolated S₁ Fragments
(P, 375X)

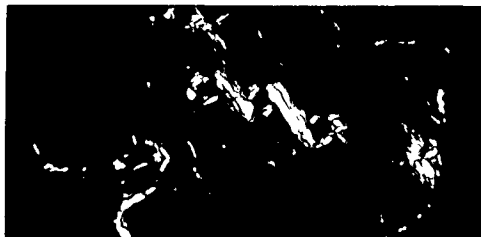


Figure 25
Isolated S₁ Fragments
(P, 375X)

agreement with the value of $62.7^\circ \pm 21.6^\circ$ determined for Pinus patula and P. caribaea by Emerton and Goldsmith (6).

POLARIZING MICROSCOPE

Unravelled P, S₁, and S₂ material was readily identifiable between the crossed nicols of a Zeiss Polarizing microscope (see Figures 21-25). When a first-order quartz red plate was inserted between the nicols, the fibers and the unravelled material exhibited retardation colors. The retardation colors are related to the thickness of doubly-refracting materials through their birefringency. This relationship was utilized to estimate the thickness of the fibers and the unravelled material. A brief discussion of the theory of this relationship is presented in Appendix II; for a more detailed discussion, see references (48) or (49) or any text on physical optics.

The birefringencies of the reclassified fibers and the unravelled S₂ layers were determined by measuring their indices of refraction (n_y) parallel, and (n_x) perpendicular to the longitudinal fiber axis by the line of Becke method with a series of Cargille liquids (48). The details of the line of Becke method are presented in Appendix III.

The indices of refraction of the reclassified fibers were measured precisely, but the thinness of the S₂ layers greatly reduced the precision of their n measurements. It is believed that the birefringency determined for the unravelled S₂ layers is reasonably accurate because it is about equal to the birefringency of the reclassified fibers. n_y, n_x, and the birefringencies of the fibers and unravelled S₂ layers are presented in Table I.

TABLE I

INDICES OF REFRACTION OF FIBERS AND S_2 LAYERS

	n_y	n_u	Birefringency
Reclassified fibers	1.584	1.526	0.058
S_2	1.59	1.53	0.06

The thicknesses of the fibers and of the unravelled material were calculated from the equation $d = R/(n_y - n_u)$; d is the thickness of the double refraction material in $m\mu$ (millimicrons), and R is its retardation in $m\mu$. The value $(n_y - n_u) = 0.06$ was used in all calculations. The retardation values, R , were determined from Newton's Color chart (49). The R values were approximations at best because they were determined by visual comparisons.

The fibers and unravelled materials produced one series of colors by increasing the retardation of the quartz plate and another series by decreasing it. The retardation of the quartz plate was 540 $m\mu$. The observed colors and the calculated thicknesses are presented in Table II.

The wall thicknesses calculated for the reclassified fibers agree with values for spruce reported by Meier (19) and by Bartunek (31). It is therefore concluded that the technique outlined above for measuring thicknesses of cellulosic materials is reasonably accurate.

The thickness of S_1 , 0.5 μ , is considerably larger than the value, 0.11-.18 μ , reported by Emerton and Goldsmith (6) for P. patula and P. caribaea. These workers estimated the thickness of S_1 "by measuring,

TABLE II

RETARDATION COLORS AND CALCULATED THICKNESSES OF FIBERS
AND UNRAVELLED MATERIAL

	Retardation Colors Greater Than 540 m μ	Retardation Colors Less Than 540 m μ	Thickness, μ
Reclassified springwood fibers	1st order blue, greenish-blue	1st order brownish- yellow, bright yellow	fiber wall, 1-2 μ
Reclassified summerwood fibers	1st order blue, green; 2nd order yellow, orange, red, and violet	retardation of fibers as large as that of plate	fiber wall, 2-6 μ
<u>P</u> Fragments	centers 1st order indigo, blue; fibrils purple, violet	centers 1st order brownish-yellow; fibrils reddish- orange	centers 1 μ , fibrils .5 μ
<u>S</u> ₁ Fragments	1st order purple, violet	1st order reddish-orange,	~.5 μ
Pit domes attached to <u>S</u> ₁ fragments	1st order purple, indigo, blue	1st order reddish-orange, brownish-yellow bright yellow	.5-2 μ
Unravelled <u>S</u> ₂ layers	1st order purple, indigo	1st order reddish-orange brownish-yellow	.5-1 μ
<u>S</u> ₂ Wall sections	centers 1st order blue, green; attached <u>S</u> ₂ layers purple	centers 1st order yellow; attached <u>S</u> ₂ layers reddish- orange	centers 2-3 μ ; attached <u>S</u> ₂ layers, ~5 μ

with a travelling microscope, the length of its shadow in the appropriate direction and multiplying this by the tangent of the angle of shadowing measured with respect to the slide." The values 0.11-.18 and .5 μ may represent a real difference in the thickness of S₁ of the two species.

On the other hand, the difference may be due to the magnitude measured. In this investigation, the thickness of S_1 was measured at the centers of the fragments where the colors were most distinct. In Emerton's study, the thickness of the S_1 fragments was measured at their edges. The edges are lines of failure where S_1 may be thinner or where it may have torn in a ragged manner; i.e., only one set of fibrils may be present. In any case, Emerton's value does not hold for white spruce because cellulose 0.11-.18 μ thick would cause a retardation of 7-11 $m\mu$. Retardations of this magnitude would not cause the colors observed.

The thickness of the centers of most P fragments, 1 μ , appears to be too large to be a true measure of the average thickness of P . The centers of the P fragments may be the thickenings in P observed by Bailey (16). On the other hand, they may have been formed by the collapse or flocculation of the sieve-forming microfibrils of P membranes during drying, or by the flocculation of several P membranes and fibrils.

PHASE CONTRAST MICROSCOPE

The fibers and the unravelled materials were examined with an American Optical Co. phase contrast microscope. The same structural details were visible as with the metallurgical microscope, although not as clearly. Figure 26 shows isolated S_1 fragments which are best identified by their dentated edges when their fibrillar orientation is not visible. At higher magnifications, the fibrils of the S_1 fragments were discernible. Because structural details were clearer when viewed with the metallurgical microscope, the phase microscope was not used much.



Figure 26
Isolated S_1 Fragments
(F*, 200X)

OTHER MICROSCOPES

The S_1 fragments were visible and identifiable by their dentated edges under the polarizing microscope with the nicols removed and the condenser iris diaphragm stopped down as far as possible. However, no structural details were visible.

Unfortunately, an interference microscope was not available for this investigation. It is possible that more precise thickness measurements could be made with it than with a polarizing microscope. Heyn (50) has reported that birefringencies can be measured precisely with the interference microscope. Lange and Kjaer (24) reported that the lignin distribution across the wall of individual fibers can be determined accurately with it.

* Photomicrograph taken with phase contrast microscope

The microfibrillar structure of S_1 and particularly S_2 has been studied extensively with the electron microscope; these investigations are too numerous to elaborate here. Emerton, et al., (51) recently obtained beautifully detailed photomicrographs of whole fibers with a reflection electron microscope. A similar investigation on isolated P and S_1 fragments may reveal much about their structure.

ESTIMATION OF MASS OF FIBERS IN P AND S_1

The fraction of the reclassified fibers' mass contained in S_1 cannot be determined with any degree of accuracy because of the great variations in fiber-wall dimensions (31). However, it can be shown from fiber models that the fraction is appreciable; it is largest in thin-walled springwood fibers and smallest in thick-walled summerwood fibers. For purposes of illustration, the fraction of the fiber mass contained in S_1 was calculated for four fiber models. It was assumed that the fibers were dry and their density uniform, that they were square-shaped and 30μ on a side, and that their lumena were square-shaped. For the models where S_2 was 1μ and 6μ thick, and S_1 0.5μ thick, the percentages of the fiber mass in S_1 were 35 and 10%, respectively. For the same dimensions of S_2 , but where S_1 was 0.15μ thick, the percentages of the fiber mass in S_1 were still appreciable, 14 and 3%, respectively. From these calculations, it was estimated that S_1 contained 5 to 15% of the mass of unbleached spruce sulfite fibers.

The P probably contains a smaller fraction of the mass of unbleached spruce sulfite fibers than S_1 for two reasons: (1) P is as thin as, or

thinner than, \underline{S}_1 . (2) The microfibrils in \underline{P} are less densely packed than in \underline{S}_1 . Therefore, it is more difficult to determine the fraction of the fibers' mass in \underline{P} than in \underline{S}_1 and no approximation was made. However, it was estimated that \underline{P} and \underline{S}_1 together contain between 5-20% of the mass of unbleached spruce sulfite fibers. This estimate was based on the 3.3% yield of $\underline{P-S}_1$ material isolated, on the observed quantities of \underline{P} and \underline{S}_1 fragments removed by classification at 30,000, 50,000 counts, etc., and on the calculations on the model fibers.

CHEMICAL ANALYSES

It was pointed out on page 25 that \underline{P} and \underline{S}_1 were essentially removed from the 300,000-count fibers and therefore these fibers are referred to hereafter as \underline{S}_2 material. An attempt was made in the chemical analyses to balance the constituents of the $\underline{P-S}_1$ and \underline{S}_2 materials with those of the reclassified fibers. In many cases, the constituents which were less concentrated in the $\underline{P-S}_1$ material than in the reclassified fibers were most concentrated in the \underline{S}_2 material. However, this relationship did not hold quantitatively, probably because a large proportion of \underline{S}_2 as well as \underline{P} and \underline{S}_1 had been removed from the 300,000-count fibers. Therefore, differences between the analyses of the reclassified fibers and the \underline{S}_2 material may reflect in part small nonuniformities in the distribution of the constituents within \underline{S}_2 .

HYDROLYSIS

The reclassified fibers, the $\underline{P-S}_1$ material, and the \underline{S}_2 material were hydrolyzed by the Forest Products Laboratory procedure (52). The samples

were treated with 72.0% sulfuric acid (3 ml./0.1 g. cellulose) at 30°C. for one hour. After diluting the sulfuric acid to 3%, the samples were autoclaved at 15 p.s.i. for one hour. The residues of the hydrolyses were filtered on microgooch crucibles and weighed. All of the weighings were made on a Kuhlman microbalance.

The acid-insoluble residues, hereafter referred to as F.P.L. Lignins, were undoubtedly similar to the "lignins" prepared by other acid hydrolysis procedures. Therefore, the results obtained here are comparable qualitatively with the lignin analyses of other investigators. The percentages of F.P.L. lignin are tabulated with the sugar analyses in Table III, and the original data are presented in Appendix V.

Although there was some variance among the F.P.L. lignin values of the P-S₁ samples, all of the values were orders-of-magnitude larger than the F.P.L. lignins of the reclassified fibers and the S₂ material. It is concluded that the concentration of lignin in P and S₁ of unbleached spruce sulfite fibers is 10 to 20 times as large as in S₂. This ratio is of the same magnitude as the one that Jayme and von Kuppen (3) determined indirectly for a sulfite pulp whose total Halse lignin content was 3.6%. Therefore, their conclusion that the relatively high concentration of lignin in P-S₁ of unbleached spruce sulfite fibers reduces the amount of interfiber bonding appears to be valid.

SUGAR ANALYSES

The sugars obtained from the acid hydrolyses were determined quantitatively by the paper chromatographic technique of Dubey (53). This

procedure is described in Appendix IV. The results of the analyses are presented in Table III and the original data in Appendix V. No arabinose, galactose, or uronic acids were found.

The sugar analysis of the reclassified fibers agrees with results obtained by Sundman, *et al.*, (54) on unbleached spruce sulfite pulps whose Halse lignin content ranged from 0.7-1.9%.

TABLE III

F.P.L. LIGNIN AND SUGAR ANALYSES

	F.P.L. lignin, %	Glucose, %	Mannose, %	Xylose, %
Reclassified fibers	0.5	89.9	6.5	3.1
<u>P-S₁</u> material	5.8	85.9	5.3	3.0
<u>S₂</u> material	0.4	86.1	9.6	3.9

Glucose, mannose, and xylose were present in the P-S₁ material and in the reclassified fibers in essentially the same ratio, 29:2:1. Therefore, the concentrations of the sugars in P and S₁ were slightly lower than in S₂ (because of the relatively high lignin concentration in P and S₁).

The mannose concentration of the S₂ material appeared to be higher than one would expect on the basis of its concentration in the reclassified fibers and the P-S₁ material. It is doubtful that this result is due to experimental error because the hemicellulose determinations also indicated that the S₂ material had a high concentration of noncellulosic

carbohydrates. This result is partly due to the higher mannose concentration in S_2 . It is also possible that, to a small extent, the mannose is distributed nonuniformly within S_2 in a manner which cannot be determined from the available data.

It has been proposed that the mannoglucans obtained from the cuprammonium-insoluble fraction of unbleached spruce sulfite pulps originate primarily from P and S_1 (55, 56). The mannose of this fraction may represent less than 20% of the mannose available in the pulp (57). P and S_1 may contain up to 20% of the mannose available in unbleached spruce sulfite fibers. Therefore, it is possible that the cuprammonium-insoluble mannoglucans originated primarily from P and S_1 , even though the over-all glucose-to-mannose ratio of P and S_1 is 16:1.

ALPHA-CELLULOSE AND HEMICELLULOSE DETERMINATION

The alpha-cellulose contents of the reclassified fibers, the $P-S_1$ material, and the S_2 material were determined by Institute Method 421 (58). The samples were treated with 17.5% sodium hydroxide at 20°C. for 45 minutes. The alpha-celluloses of the fibers were white, and the alpha-cellulose of the $P-S_1$ material was light brown. Because the $P-S_1$ material contained 5.8% lignin, the F.P.L. lignin content of its alpha-cellulose was determined. It was found to be 5.6%, which is equal to 4.8% of the weight of the $P-S_1$ material.

The filtrates from the alpha-cellulose determinations contained the hemicelluloses soluble in 17.5% sodium hydroxide, hereafter referred to

as the hemicelluloses. The filtrates from the fibers were colorless, but the one from the P-S₁ material was slightly yellow. It contained a small amount of lignin calculated by difference to be equal to 1.0% of the P-S₁ material.

The results of the alpha-cellulose and hemicellulose determinations are presented in Table IV and the original data in Appendix V.

TABLE IV

ALPHA-CELLULOSE AND HEMICELLULOSE ANALYSES

	Alpha- cellulose, %	Hemi- cellulose, %	F.P.I. Lignin, %
Reclassified fibers	84.0	15.5	0.5
<u>P-S₁</u> Material	81.3	12.9	5.8
<u>S₂</u> Material	82.6	17.0	0.4

The concentrations of the alpha-cellulose and the hemicelluloses in P and S₁ were 2.7 and 2.6% lower respectively than in the reclassified fibers. These data demonstrate that the concentration of the hemicelluloses is slightly higher in S₂ than in P and S₁. Therefore, the hemicellulose and lignin distributions across the wall of unbleached spruce sulfite fibers are not alike as hypothesized by Jayme and von Köppen (3) and the conclusions based on their assumed hemicellulose distribution are in doubt (see page 11).

It may be postulated that the lignin in the P-S₁ material prevented a portion of the hemicelluloses from dissolving in the 17.5% sodium

hydroxide because of the hypothesized lignin-hemicellulose bond (2). Holocelluloses from which the hemicelluloses are normally extracted contain 2-4% Klason lignin, a quantity which is not too much smaller than the lignin content of P and S₁ (57). Furthermore, the sugar analysis also showed that the concentration of noncellulosic carbohydrates in P and S₁ was lower than in S₂. Therefore, the lignin in P and S₁ could hardly have prevented more than a very small fraction of the hemicelluloses, if any at all, from dissolving in the 17.5% sodium hydroxide.

DEGREE OF POLYMERIZATION

The degree of polymerization (D.P.) of the reclassified fibers, the P-S₁ material, and the S₂ material was calculated from the intrinsic viscosity measurements made on the nitrated samples. The samples were nitrated with a 43:32:25 nitric acid, acetic acid, acetic anhydride mixture at 3°C. for three hours to produce cellulose nitrates, assumed to contain 13.8-13.9% nitrogen. This assumption was based on two sources: (1) Swensen (59) found that this particular nitrating agent produces cellulose nitrates with a nitrogen content of 13.8 to 13.9%. (2) Lindsley and Frank (60) have shown that the composition of the nitrating agent determines the degree of substitution of pulps.

After the yields of the nitrations were determined, the samples were dissolved in ethyl acetate at a concentration of 0.05 g./100 ml. and allowed to stand overnight. Eight milliliters of each solution were pipetted, in turn, into a Cannon-Fenske viscometer mounted in a 25°C.

constant-temperature bath. Viscosity measurements were made on the undiluted samples and after dilution with 4, 8, and 12 ml. of ethyl acetate. The intrinsic viscosities, $[\eta]$, were determined in the usual manner from the specific viscosity-concentration curves (61). The D.P.'s were calculated from the $[\eta]$'s by Hunt's equation, $[\eta] = 2.50 \times 10^{-5} (\overline{M}_w)^{1.01}$, where \overline{M}_w is the molecular weight of the cellulose nitrate (61). The constant of this equation was determined for solutions of cellulose nitrate, containing 13.5% nitrogen, in ethyl acetate by the osmotic pressure, light scattering, and other molecular weight-determination methods (61). The appropriate corrections were applied to the $[\eta]$'s by the equation of Lindsley and Frank (60) to account for the difference in the nitrogen content obtained in this investigation and by Hunt.

The yields of the nitrations, the $[\eta]$'s and the D.P.'s are presented in Table V and the original data in Appendix V.

TABLE V

DEGREE OF POLYMERIZATION DATA

	Yields of Nitration, %	Intrinsic Viscosity	Average D.P. (61)
Reclassified fibers	93.5	27.0	2960
<u>P-S</u> ₁ Material	90.4	18.5	2030
<u>S</u> ₂ Material	94.5	27.0	3050

The difference between the D.P.'s of the reclassified fibers and the S₂ material is so small that the D.P. of S₂ must be around 3000. It is

therefore concluded that in unbleached spruce sulfite fibers, the D.P. of \underline{P} and \underline{S}_1 is about two thirds of that of \underline{S}_2 .

Jayme and von Köppen (3) indicated that the D.P. of \underline{P} and \underline{S}_1 of unbleached spruce sulfite fibers was about 300. (See page 11.) They concluded that the low D.P. of \underline{P} and \underline{S}_1 is partially responsible for the inferior strength properties of sulfite fibers. Because carbohydrates with a D.P. over 2000 certainly are not short-chained, it is believed that Jayme and von Köppen's conclusion is in doubt.

The maximum D.P. of the hemicelluloses soluble in 17.5% sodium hydroxide is about 250* (62), a value which is less than one sixth of the average D.P. of the $\underline{P-S}_1$ material. Therefore, the differences in the D.P.'s of the three samples should hardly be reflected in their solubilities in 17.5% sodium hydroxide.

DEGREE OF CRYSTALLINITY

The degree of crystallinity of the reclassified fibers and the $\underline{P-S}_1$ material was determined from diffraction patterns recorded by a North American Phillips Co. x-ray unit. The samples were prepared as follows:

The reclassified fibers and the $\underline{P-S}_1$ material were ground up in a micro-Wiley mill. The materials passing through the 40-mesh screen were formed in a Carver Press into one-inch diameter disks each weighing 0.248 g. The thicknesses of the reclassified fibers and the $\underline{P-S}_1$ disks were 0.0210 in. and 0.0231 in., respectively.

*The D.P. reported in (62) is 200. It was calculated by Staudinger's equation and was recalculated here by Hunt's equation (61).

Although the over-all density of the cellulose samples has an effect on the x-ray diffraction patterns, Wiberg (63) has shown that a density difference like the one obtained in this investigation has a negligible effect.

The disks were mounted in an aluminum holder flush with its top surface. The x-ray diffraction patterns were recorded under the following conditions:

Radiation: CuK_α (nickel filter). $\lambda = 1.54 \text{ \AA}$.

Divergence slit: 0.5° .

Scatter slit: 0.006 in.

Receiving slit: 0.5° .

Voltage: 35 kv.

Current: 20 ma.

Scanning rate: $0.25^\circ/\text{min}$.

The diffraction patterns were recorded between $2\theta = 11$ and 27° ; 2θ is the total deflection of the x-ray. The intensity of a standard aluminum alloy at $2\theta = 38.4^\circ$ was determined immediately before and after each recording to check the performance of the instrument. The x-ray diffraction patterns are shown in Figure 27.

The degree of crystallinity of a pulp is a function of the size, number, and internal degree of order of its micelles, of its over-all density, and of its concentration of noncellulosics. It is probable that the relatively high concentration of lignin in the P-S_1 material

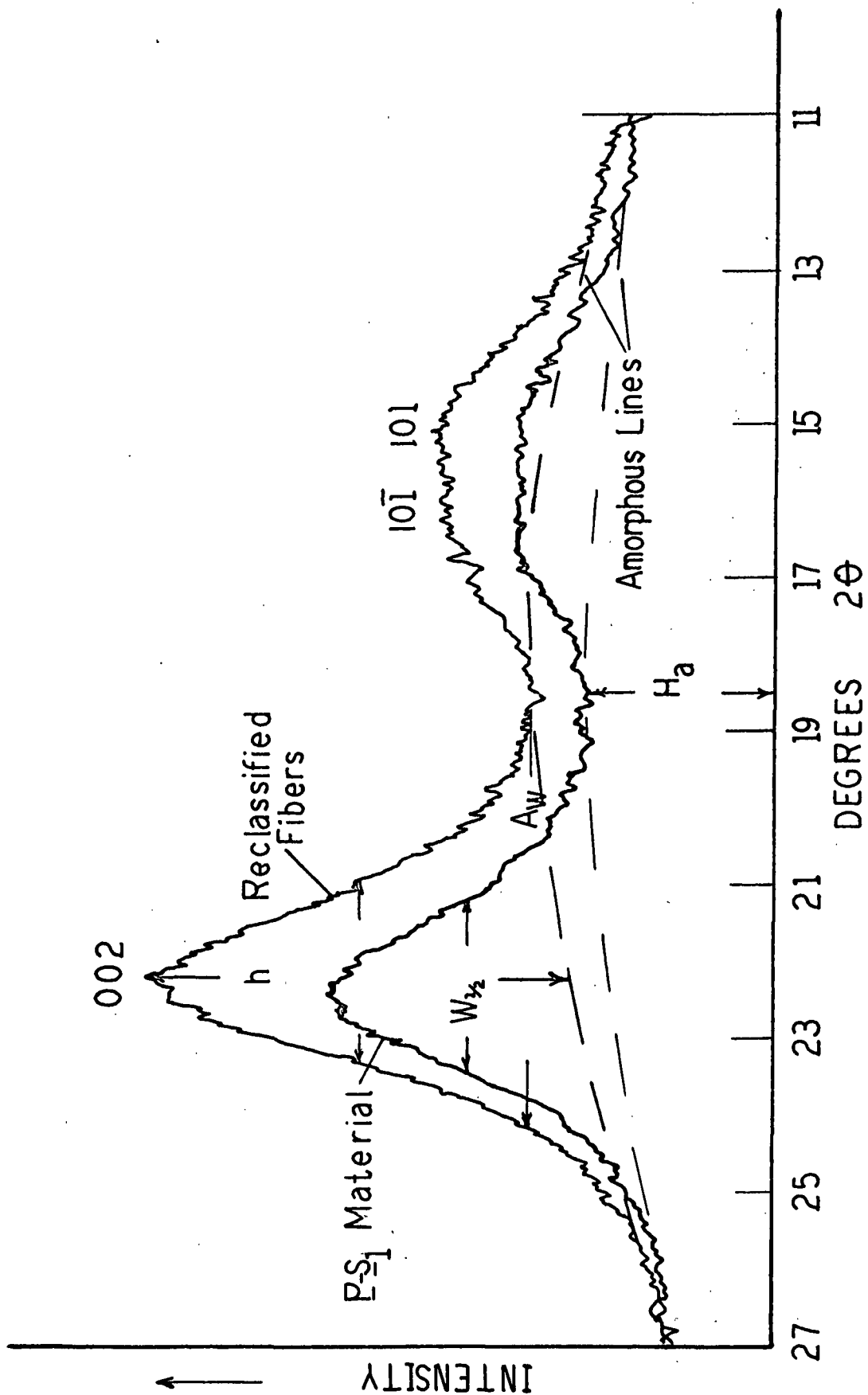


Figure 27

X-ray Diffraction Patterns of Reclassified Fibers
and P-S₁ Material

decreased its apparent crystallinity somewhat. The $\underline{P-S}_1$ material was not delignified because it was saved for other analyses.

The interpretation of x-ray diffraction patterns has not yet been fully worked out, although numerous equations for determining "per cent crystallinity" have been proposed. In general, the investigators in the field agree that the degree of crystallinity of cellulose is a function of the height of the 002 peak. However, it has been proposed that the degree of noncrystallinity is a function of \underline{H}_a (64), \underline{A}_w (65), and $\underline{W}_{1/2}$ (63). The dimension $\underline{W}_{1/2}$ was selected for this investigation because it has a theoretical basis (65).

The degree of crystallinity of the samples was ranked by the equation "crystalline ranking" = $\underline{h}/\underline{W}_{1/2}$ (63) (Figure 27); \underline{h} was measured in scale units and $\underline{W}_{1/2}$ in degrees 2θ . The crystalline ranking of the reclassified fibers was 11.7 and that of the $\underline{P-S}_1$ material, 7.8.

It is concluded that \underline{P} and \underline{S}_1 of unbleached spruce sulfite fibers are partially crystalline, but not as crystalline as \underline{S}_2 . It is not known whether the difference between the crystallinity of $\underline{P-S}_1$ and \underline{S}_2 is due only to the relatively high lignin concentration of the $\underline{P-S}_1$ material, or also to a small difference in the degree of crystallinity of their cellulosic portions.

IMPORTANCE OF UNRAVELLED \underline{P} AND \underline{S}_1 FRAGMENTS TO SHEET STRENGTH PROPERTIES

It was demonstrated in the following experiment that unravelled \underline{P} and \underline{S}_1 fragments can exert a considerable influence on sheet strength properties

by acting as a bonding agent. Reclassified fibers, which had been stirred 1200 counts instead of 2500 in their initial preparation, were stirred a total of 15,000 counts in the British disintegrator and then classified to remove the unravelled \underline{P} and \underline{S}_1 fragments. The physical properties and the sheet strength properties of the reclassified fibers, (A), the 15,000-count fibers, (B), and the classified 15,000-count fibers, (C), were measured.

The handsheets were prepared according to Institute Method 411 (58) and tested according to the Institute Methods listed in Table VI. The filtration specific surface and the wet fiber specific volume data were determined by the filtration resistance technique of Ingmanson (66).

In the analysis of the data, two assumptions were made: (1) a negligible quantity of \underline{P} and \underline{S}_1 fragments were lost during the formation of the handsheets of the 15,000-count fibers. (2) The four-minute classification had a negligible effect on the properties of the 15,000-count fibers. Therefore, the differences between the properties of the 15,000-count fibers and the classified 15,000-count fibers were due primarily to the unravelled \underline{P} and \underline{S}_1 fragments. If \underline{X} is a specific property, the fraction of the total change in \underline{X} which can be attributed to the presence of unravelled \underline{P} and \underline{S}_1 fragments is $(\underline{X}_B - \underline{X}_C)/(\underline{X}_B - \underline{X}_A)$; the fraction of the change due to all other effects combined is $(\underline{X}_C - \underline{X}_A)/(\underline{X}_B - \underline{X}_A)$. It should be pointed out that the first of these two equations is applicable only in cases where the changes in the sheet's properties can be attributed to a specific cause.

TABLE VI

PHYSICAL PROPERTIES AND SHEET STRENGTH PROPERTIES
OF STIRRED FIBERS

Property	Reclassi- fied Fibers (A)	15,000- Count Fibers (B)	Classi- fied 15,000- Count Fibers (C)	Classified 300,000- Count Fibers
Filtration specific surface, cm. ² /g.	10,780	38,400	17,000	70,800
Wet fiber specific volume, cc./g.	0.96	3.21	3.29	3.88
Basis weight, ^a lb./25 x 40 x 500	51.8	51.3	51.5	39.8
Apparent density, ^b lb./ream mil	12.9	16.1	15.2	16.6
Bursting strength, ^c pts./100 lb.	109	169	153	102
Tensile strength, ^d lb./in.	29.9	42.7	34.6	14.4
Tear factor, ^e	1.68	1.10	1.24	1.04
M.I.T. fold ^f	1093	2060	1419	1733
Zero span tensile ^g strength, lb./in	72.0	61.5	60.7	48.8

The handsheets were tested by the following Institute Methods:

- ^a Basis weight, 504
- ^b Apparent density, 508
- ^c Bursting strength, 510
- ^d Tensile strength, 511
- ^e Tearing strength, 512
- ^f M.I.T. fold, Part II, 513
- ^g Zero-span tensile strength, (70) (IPC jaws)

The properties of the classified 300,000-count fibers were measured to show the effects of prolonged stirring on the properties of the reclassified fibers. Differences between the properties of these two types of fibers cannot be attributed to any specific phenomenon, but only to a general maceration of the fibers.

From the filtration specific surface and the wet fiber specific volume, it is evident that 13,800 counts of stirring created a considerable amount of hydrodynamic surface, 27,620 sq. cm./g., and caused appreciable fiber swelling. Most of the newly created surface, 77.4% ($21,400 \text{ cm.}^2/\text{g.} / 27,620 \text{ cm.}^2/\text{g.} \times 100$), was due to the unravelled P and S₁ fragments which comprised only 3.3% of the mass of the reclassified fibers. The unravelled P and S₁ fragments had a hydrodynamic surface of about 650,000 sq. cm./g. ($21,400 \text{ cm.}^2 / .033 \text{ g.}$). A fine, fibrous material with a specific surface of this magnitude should enhance interfiber bonding considerably.

The contribution of the unravelled P and S₁ fragments, and of all other effects combined, to the strength properties developed by the reclassified fibers during the first 13,800 counts of stirring are tabulated in Table VII.

The differences in the strength properties between the 15,000-count fibers and the classified 15,000-count fibers were appreciable. The decreases in the apparent density, bursting strength, tensile strength, and fold and the increase in the tearing strength, caused by the removal of the P and S₁ fragments, indicate that the unravelled P and S₁ fragments acted as bonding agents.

TABLE VII

PER CENT OF STRENGTH PROPERTY INCREASES DUE TO UNRAVELLED
P and S₁ FRAGMENTS AND DUE TO OTHER EFFECTS COMBINED

Property	Per Cent of Increase Due to Unravelled <u>P</u> and <u>S₁</u> Fragments	Per Cent of Increase Due to Other Effects Combined
Apparent density	28	72
Bursting strength	27	73
Tensile strength	63	37
Fold	66	34
Tearing strength	-24	-76

The unravelled P and S₁ fragments were particularly important in the development of the tensile strength and folding endurance during the first 13,800 counts of stirring of the reclassified fibers. The contribution of the unravelled P and S₁ fragments to these two strength properties was about 1.7 and 1.9 times, respectively, as large as that of all other effects combined.

The reclassified fibers had exceptionally high strength properties for an essentially unbeaten, unbleached spruce sulfite pulp. The high strength properties were due primarily to the absence of cut fibers, pulping debris, and the minimal fiber damage during the pulp preparation. The data point out the excellent strength properties inherent in unbleached spruce sulfite fibers.

The relatively high apparent density and M.I.T. fold of the 300,000-count fibers suggest that the extent of interfiber bonding was greater

among these fibers than among the reclassified and 15,000-count fibers. However, the extensive damage to the 300,000-count fibers caused their other strength properties to be lower than those of the other fibers. This damage was evident from the lower zero-span tensile strength and from microscopic examinations.

Jayme and von K⁸ppen (3) indicated that the lignin present in P and S₁ of unbleached spruce sulfite fibers reduces the amount of interfiber bonding. In view of the contribution made by unravelled P and S₁ fragments to sheet strength properties in this investigation, it is conceivable that P and S₁ fragments delignified further by bleaching, but otherwise not greatly degraded, may have an even larger effect on sheet strength properties.

SWELLING OF FIBERS

The role of P and S₁ during the swelling of fibers has been studied for many years. The generally accepted mechanism of fiber swelling postulated by Wardrop and Dadswell (56) and by Steenberg (67) is as follows:

Upon the application of a swelling agent, the fiber first swells uniformly, but its expansion is soon restricted by P and S₁. As the concentration of the swelling agent is increased, swelling of S₂ proceeds at the slip planes. The slip planes are cracks in P and S₁ caused by the bending or bruising of fibers. [If sufficient mechanical treatment is applied to a fiber, S₂ appears to swell somewhat at the original slip planes prior to the application of the swelling agent (Figure 28).]

During the swelling of S_2 at the slip planes, S_1 is stretched, and it contracts perpendicularly to its fibrillar orientation. Wherever S_1 has slipped from its surface, S_2 expands still further and forms the renowned balloons (Figures 29 and 30). When the swelling of S_2 is at its maximum, just prior to its dissolution, S_1 is present about the fiber as a band which forms nodes at regular intervals (Figure 30). P may remain attached to S_1 , but more generally it is split from the fiber and floats away. If the concentration of the swelling agent is increased still further, S_2 dissolves. Whether or not P and S_1 also dissolve depends on their chemical composition.

Wardrop and Dadswell (56) concluded from their studies on ballooning "that in coniferous tracheids the layer responsible for the constrictions formed between the balloons which arise from the middle secondary wall (S_2), is the outer layer of the secondary wall (S_1). The primary wall may also participate in the formation of the constrictions, but usually this layer is detached during the progress of swelling." Therefore, it was hypothesized that if P and S_1 were removed from the fibers without any concurrent chemical changes, the fibers ought to swell uniformly until they dissolved.

It was believed that P and S_1 were essentially removed from the 300,000-count fibers because only trace quantities of P - S_1 material were unravelled between 200,000 and 300,000 counts. Therefore, the reclassified fibers and the 300,000-count fibers which appeared to be intact were well-suited to test the hypothesis presented above. They were treated

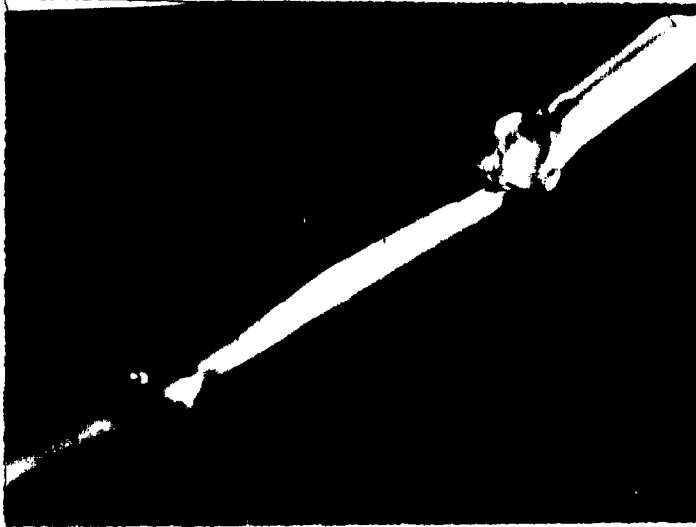


Figure 28
300,000-count Fiber
(P, 190X)



Figure 29
Swollen Reclassified Fiber
(P, 190X)

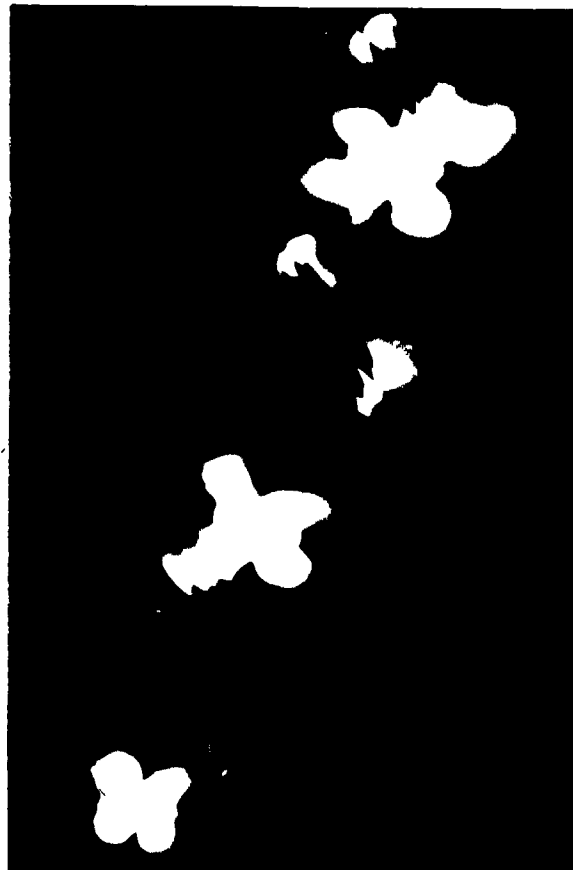


Figure 30
Swollen Reclassified Fiber
(P, 190X)

with cupriethylenediamine in a cardioid cell under the polarizing microscope according to the procedure of Isenberg and Smith (69).

The reclassified fibers ballooned normally. The 300,000-count fibers swelled without any apparent constrictions (Figure 31). Before finally dissolving, the springwood fibers swelled two to four times their original diameter and the summerwood fibers three to six times. The fibers also underwent considerable lengthwise shrinkage. This shrinkage could not be measured because one end of the fibers would dissolve before the other had undergone its full contraction.

The fibrils of the swollen 300,000-count fibers appeared to be oriented almost at right angles to the longitudinal fiber axis (Figure 31). The orientation of the S_2 fibrils apparently was altered by the swelling and the contraction of the fibers.

A small fraction of the 300,000-count fibers retained a portion of their S_1 intact and underwent partial ballooning like the fiber in Figure 32. The stage of swelling of this fiber increases sixfold from left to right because there was a concentration gradient of the swelling agent across the cell.

The manner in which the reclassified fibers and the 300,000-count fibers swelled is consistent with the concept that S_1 forms the constrictions during ballooning. Therefore, the conclusion of Wardrop and Dadswell (56) concerning the role of S_1 during ballooning has been confirmed.



Figure 31
Swollen 300,000-count Fiber
(P, 190X)



Figure 32
Swollen 300,000-count Fiber
(P, 190X)

During the 1930's, it was believed that the balloons were covered with a "skin substance" or "sheath," presumably \underline{P} , where \underline{S}_1 had slipped from the surface of \underline{S}_2 (34). It was believed that the "skin substance" prevented \underline{S}_2 from dissolving until the concentration of the swelling agent was high enough to crack the skin, whereupon \underline{S}_2 dissolved. Although this concept has been rejected by Wardrop and Dadswell (56) and by Merler and Wise (55), the existence or nonexistence of the "skin substance" has never been definitely established one way or the other.

If the "skin substance" does not exist, \underline{S}_2 must be in direct contact with the swelling agent at the balloons. For this case, Steenberg (67) hypothesized that the dissolution of \underline{S}_2 represents a phase change from a swollen gel to complete solution. He supported this hypothesis by demonstrating that highly swollen fibers dissolve when the concentration of the swelling agent is increased only very slightly.

If the dissolution of \underline{S}_2 represents a phase change, intact fibers and fibers from which \underline{P} and \underline{S}_1 have been removed ought to dissolve at the same concentration. On the other hand, if a "skin substance" prevents the dissolution of the ballooned fibers, the fibers from which \underline{P} and \underline{S}_1 have been removed ought to dissolve at a lower concentration than the ballooning fibers. This hypothesis was tested by swelling the reclassified fibers and the 300,000-count fibers together. It was found that both dissolved at the same concentration. Wall sections like the swollen one shown in Figure 33 also dissolved at the same concentration as the reclassified fibers. These observations confirm the conclusion of

Wardrop and Dadswell (56) that there is "no necessity to postulate the existence of a membrane between the solvent and the cellulose gel to account for the existence of the latter as a separate phase".



Figure 33
Swollen S_2 Wall Section
(P, 190X)

CONCLUSIONS

A technique has been developed for isolating $\underline{P-S_1}$ material and $\underline{S_2}$ material from unbleached spruce sulfite fibers in sufficiently large quantities for chemical analyses. The isolation of the $\underline{P-S_1}$ and the $\underline{S_2}$ materials requires only readily available equipment and it is a relatively simple and rapid technique. From the analyses of the $\underline{P-S_1}$ and $\underline{S_2}$ materials and the original fibers, it is possible for the first time to approximate the distribution of the constituents across the wall of delignified fibers.

The distribution of the constituents across the wall of unbleached spruce sulfite fibers has been determined to be as follows:

The concentration of lignin in \underline{P} and $\underline{S_1}$ is 10 to 20 times as large as in $\underline{S_2}$ (Ca. 5.8% versus 0.4%). This finding substantiates a similar one obtained by Jayme and von Köppen (3). Therefore, their conclusion that the relatively high concentration of lignin in \underline{P} and $\underline{S_1}$ of unbleached spruce sulfite fibers reduces the amount of interfiber bonding appears to be valid.

The carbohydrates are distributed much more uniformly across the fiber wall than postulated by Jayme and von Köppen (3). Contrary to their well-known assumption that the hemicellulose and lignin distributions are alike, it was found that the concentration of hemicelluloses in \underline{P} and $\underline{S_1}$ (12.9%) is slightly lower than in $\underline{S_2}$ (15.5-17.0%). The distribution of the hemicelluloses is consistent with the distribution of the

sugars, glucose, mannose, and xylose, which are present in an essentially constant ratio (29:2:1) across the fiber wall. The concentration of alpha-cellulose in P and S₁ (81.3%) is slightly lower than in S₂ (82.6-84.0%). The D.P. of P and S₁, 2030, is about two thirds of that of S₂. This finding demonstrates that P and S₁ are not composed of short carbohydrate chains with an average D.P. of 300 as postulated by Jayme and von Köppen (3). P and S₁ are partially crystalline, but not as much as S₂. It was not determined whether this difference is due only to the relatively high concentration of lignin in P and S₁, or also due to a real difference in the crystallinity of the carbohydrates in P and S₁, and in S₂.

It is concluded that the strength of the interfiber bonds between unbleached spruce sulfite fibers is not reduced appreciably by a high concentration of hemicelluloses and low D.P. cellulose in P and S₁ as proposed by Jayme and von Köppen (3).

The thickness of S₁ was found to be about 0.5 μ . The yield of P-S₁ material isolated was 3.3% of the weight of the reclassified fibers. On the basis of these findings, it is concluded that P and S₁ together contain between 5 and 20% of the mass of unbleached spruce sulfite fibers. This proportion is somewhat larger than has been generally realized.

The P and S₁ fragments unravelled from the reclassified fibers in the British disintegrator have a huge hydrodynamic surface, 650,000 cm.²/g. A fine, fibrous material with a specific surface of this magnitude should improve sheet strength properties considerably. Under the conditions used in this investigation, it was found that the unravelled P

and S_1 fragments were responsible for over 25% of the increase in bursting strength and for over 60% of the increase in the fold and tensile strength. Therefore, it is believed that the importance of P and S_1 to the paper-maker has been underestimated.

Two hypotheses on the mechanism of swelling were substantiated. (1) The theory of Wardrop and Dadswell (56) that S_1 is responsible for the constrictions formed during ballooning was corroborated. (2) The hypothesis of Steenberg (67) that the dissolution of ballooned fibers represents a phase change was strengthened. Therefore, it is concluded in agreement with these investigators that the "skin substance" concept is unnecessary to explain the mechanism of ballooning.

The S_2 wall unravelled in two distinctly different ways. An hypothesis is presented which relates these types of fibrillation to fiber structure.

Two controversial morphological characteristics of fibers were studied. The conclusion of Emerton and Goldsmith (6) that S_1 contains two sets of fibrils with a fibrillar angle of about 60° was confirmed for spruce. The conclusion of Wardrop and Dadswell (36) that S_2 and the layer bordering the lumen have the same fibrillar orientation was confirmed.

ACKNOWLEDGMENT

I would like to express my sincere appreciation to my advisory committee, Messrs. I. H. Isenberg, N. Jappe, E. Dickey, and M. May for their assistance and encouragment; to Appleton Wire Works for the use of their metallurgical microscope; to Mr. J. Gerhauser of the Appleton Wire Works for his assistance in using the metallurgical microscope; to Mr. G. Dubey for his assistance in the sugar analyses; to Mr. F. Sweeney and Mr. A. Schultz for their assistance in preparing the photomicrographs; and to W. Wiberg for his assistance in recording the x-ray diffraction patterns.

LITERATURE CITED

1. Graff, J. H., Paper Trade J. 117, no. 17:25-31(Oct. 21, 1943).
2. Emerton, H. W. Fundamentals of the beating process. Kenley, England. The British Paper and Board Research Assoc., 1957. 197 p.
3. Jayme, G., and Köppen, A. von. Das Papier 4, no. 19/20:373-8; no. 21/22:415-20; no. 23/24:456-62(Oct., Nov., Dec., 1950).
4. Lange, P. W., Svensk Papperstidn. 53, no. 23:749-66(Dec., 1950).
5. Clark, J. d'A., Paper Industry and Paper World 25, no. 4:382-6(July, 1943).
6. Emerton, H. W., and Goldsmith, V., Holzforschung 10, no. 4:108-15 (Sept., 1956).
7. Isenberg, I. H. Pulpwoods of the U. S. and Canada. 2nd Ed. Appleton, Wis., The Institute of Paper Chemistry, 1951. 187 p.
8. Ranby, B. Fine structure of cellulose fibrils. In Fundamentals of papermaking fibres. p. 61. Kenley, England, The Tech. Sect. of British Paper and Board Makers' Assoc., 1958.
9. Frey-Wyssling, A., Endeavour 14, no. 53:34-9(Jan., 1955).
10. Frey-Wyssling, A., Science 114, no. 3081:80-2(Jan. 15, 1954).
11. Hodge, A. J., and Wardrop, A. B., Australian J. Sci. Res. B3, no. 3: 365-9(Aug., 1950).
12. Ranby, B. G., Svensk Papperstidn. 55, no. 4:115-24(Feb., 1952).
13. Giertz, H. W., World's Paper Trade Review 138, no. 19:1451-62(Nov. 6, 1952).
14. Wardrop, A. B., Tappi 40, no. 4:225-43(April, 1957).
15. Bixler, A., Paper Trade J. 107, no. 15:29-40(Oct. 13, 1938).
16. Bailey, I. W., Ind. Eng. Chem. 30, no. 1:40-7(Jan., 1938).
17. Emerton, H. W., J. Roy. Microscopy Soc. 74, part 1:35-40(Jan., 1954).
18. Jayme, G., and Hunger, G., Holz Roh u. Werkstoff 13, no. 6:212-15(June, 1955).
19. Meier, H., Holz Roh u. Werkstoff 12, no. 9:323-38(Sept., 1955).

20. Ritter, G. J., Ind. Eng. Chem. 17:1194-7(1925).
21. Kerr, T. J., and Bailey, I. W., J. Arnold Arboretum 15:327-50(1934).
22. Bailey, A. J., Paper Industry 18, no. 5:379-81(Aug., 1936).
23. Lange, P. W., Svensk Papperstidn. 57, no. 16:563-7(Aug. 31, 1954).
24. Lange, P. W., and Kjaer, A., Norsk Skogind. 11, no. 11:425-32(Nov., 1957).
25. Giertz, H. W. The effect of beating on individual fibers. In Fundamentals of papermaking fibres, p. 397. Kenley, England, The Tech. Sect. of British Paper and Board Makers' Assoc., 1958.
26. Bailey, I. W., and Kerr, T. J., J. Arnold Arboretum 16, no. 3:273-300(July, 1935).
27. James, C. F., and Wardrop, A. B., Australian Pulp & Paper Ind. Tech. Assoc. Proc. 9:107-24(1955).
28. Meier, H., Holzforschung 11, no. 2:41-6(May, 1957).
29. Emerton, H. W., Tappi 40, no. 7:542-7(July, 1957).
30. Wardrop, A. B., Holzforschung 11, no. 4:102-10(Oct., 1957).
31. Bartunek, R., Das Papier 12, no. 1/2:14-21(Jan., 1958).
32. Dolmetsch, H., Kolloid Z. 108, no. 2/3:183-92(Aug., Sept., 1944).
33. Brauns, F. E., and Lewis, H. F., Paper Trade J. 105, no. 10:35-7(Sept. 2, 1937).
34. Strachan, J., Paper Maker and British Paper Trade J. 91, no. 3:TS 33-4(March, 1936).
35. Wardrop, A. B., and Dadswell, H. E., Holzforschung 11, no. 2:33-4(May, 1957).
36. Wardrop, A. B., and Dadswell, H. E., Australian J. Sci. Research B3, no. 1:1-13(Feb., 1950).
37. Bailey, I. W., Bull. Torrey Botan. Club 66, no. 4:201-13(April, 1939).
38. Wardrop, A. B., Holzforschung 8, no. 1:12-29(1954).
39. Lange, P. W., Svensk Papperstidn. 57, no. 15:525-32(Aug. 15, 1954).
40. Asunmaa, S., and Lange, P. W., Svensk Papperstidn. 57, no. 14:501-16(July 31, 1954).

41. Bucher, H., Assoc. tech. ind. papetière, Bull. no. 4-5:95-104(1955).
42. Asunmaa, S., Svensk Papperstidn. 8, no. 30:308-10(April 30, 1955).
43. Meier, H., and Yllner, S., Svensk Papperstidn. 59, no. 11:395-401 (June 15, 1956).
44. Bailey, A. J., Ind. Eng. Chem., Anal. Ed. 8, no. 1:52-4(Jan. 15, 1936).
45. Stemsrud, F., Norsk Skogind. 10, no. 4:123-37(April, 1956).
46. Frey-Wyssling, A., and Bosshard, H. H., Holz Roh u. Werkstoff 11, no. 11:417-20(Nov., 1953).
47. Emerton, H. W., British Paper and Board Makers' Assoc., Proc. Tech. Sect. 36:595(Dec., 1955).
48. Heyn, A. N. J. Fiber microscopy. Chapter 20, 21. New York, Interscience Publishers Inc., 1954..407 p.
49. Vickers, A. E. J. The polarizing microscope in organic chemistry and biology. In Modern methods of microscopy. p. 103. London, England, Butterworth Scientific Publications, 1956.
50. Heyn, A. N. J., Textile Research J. 27, no. 6:449-58(June, 1958).
51. Emerton, H. W., Watts, J., Amboss, K., and Simpson, A. Reflection electron microscopy of fibers: a new research method. British Paper and Board Industry Research Assoc., Physics B Dept., Ref. RA/T/38 (July, 1954).
52. Saemans, J., Moore, W., Mitchell, R., and Millett, M., Tappi 35, no. 8:336-43(Aug., 1952).
53. Dubey, G. Personal communication, 1958.
54. Sundman, J., Sarnio, J., and Gustafsson, C., Paper and Timber 53, no. 4a:115-21(1951).
55. Merler, E., and Wise, L. E., Tappi 41, no. 2:80-5(Feb., 1958).
56. Wardrop, A. B., and Dadswell, H. E., Australian Pulp & Paper Ind. Tech. Assoc. Proc. 4:198-221(1950).
57. Wise, L. E. Personal communication, 1958.
58. Institute of Paper Chemistry Methods, 1952.
59. Swenson, H. E. Personal communication, 1958.

60. Lindsley, C., and Frank, M., Ind. Eng. Chem. 45:2491-7(1953).
61. Hunt, M., Newman, S., Sherae, H., and Flory, P., J. Phys. Chem. 60:1278-90(Sept., 1956).
62. Purves, C. Chemical nature of cellulose and its derivatives. In Ott's Cellulose and Cellulose Derivatives. I. p. 93. New York, Interscience Publishers Inc., 1954.
63. Wiberg, W. Personal communication, 1958.
64. Hermans, P., and Weidinger, A., J. Appl. Phys. 19, no. 5:491-506 (May, 1948).
65. Ant-Wuorinen, O., Paperi ja Puu 37, no. 8:335-68(Aug., 1955).
66. Ingmanson, W., Tappi 35, no. 10:439-48(Oct., 1952).
67. Steenberg, B., Svensk Papperstidn. 50, no. 11B:155-63(1947).
68. Isenberg, I. H., and Smith, O., Tappi 39, no. 4:226-7(April, 1956).
69. Piper, C. V., and Bernardin, L. J., Tappi. 41, no. 1:16-19(Jan., 1958).
70. Wink, W. A. Personal communication.

APPENDIX I

PREPARATION OF PULP

Three white spruce logs* [Picea glauca (Moench) Voss] were reduced to 5/8-in. chips by a Carthage chipper. The fines were removed from the chips by a $\frac{1}{4}$ -in. mesh screen and the knots and the over-sized chips by hand. The chips were stored in polyethylene bags for one week prior to cooking.

Five thousand grams (4300 g. oven-dry) of chips were cooked in the number four digester of the pulp laboratory of the Institute. Twenty-eight liters of cooking liquor were used, giving a liquor-to-wood ratio of six to one. The composition of the cooking liquor as determined by the Palmrose titration was as follows: total SO_2 = 7.27%, free SO_2 = 6.09%, and combined SO_2 = 1.18%.

The chips were cooked in a basket mounted in the digester. They were presteamed at 40 p.s.i. for 40 minutes and allowed to cool. The liquor was added to the digester and heated indirectly from 30 to 110°C. in two hours; from 110 to 120°C. in one hour; from 120 to 131°C. in eight hours; and maintained at 131°C. for $1\frac{1}{2}$ hours. The steam was shut off, and the temperature was allowed to drop to 94°C. The digester was opened and the basket of chips removed before the liquor was discharged. The chips were treated further in the manner described on page 17.

* The logs were obtained through the courtesy of Consolidated Water Power and Paper Co., Appleton, Wisconsin.

APPENDIX II

THEORY OF THICKNESS MEASUREMENTS MADE WITH POLARIZING MICROSCOPE

When white light emerges from the polarizer of a polarizing microscope, its electric vector vibrates in a single plane. While passing through a birefringent cellulose fiber whose longitudinal fiber axis is oriented at 45° to the plane of vibration of the polarizer, this ray is resolved into two mutually perpendicular components. One of these rays vibrates parallel, and the other perpendicular to the fiber axis. The two rays pass through the fiber with different velocities because the indices of refraction in the two directions are different. Therefore, the optical path lengths are different, and the two rays are out of phase when they emerge from the fiber. The optical path length difference, or the retardation, R , is equal to $d(n_y - n_x)$. The phase difference, δ , for each wavelength, λ , is equal to $2\pi R/\lambda = 2\pi d(n_y - n_x)/\lambda$. δ is different for every wavelength.

The plane of vibration of the analyzer is perpendicular to that of the polarizer, i.e., the analyzer and the polarizer are crossed. When the two mutually perpendicular rays from the fiber strike the analyzer, only the component rays vibrating parallel to the plane of vibration of the analyzer pass through. The rays from the analyzer are still out of phase, but they vibrate in the same plane. Therefore, some of the wavelengths will interfere destructively and others constructively, giving the light leaving the analyzer a resultant

color. The hue of this color depends on the wavelength distribution of the light incident to the polarizer, the thickness, and the birefringency of the fiber. For incident white light, Newton's color scale relates the observed colors to the retardation for sodium light.

In actual practice, the retardation caused by most fibers is so small that no observable interference takes place, and the fibers are white. However, it is possible to distinguish between large retardation values which differ by a small amount, such as 540 $m\mu$ and 570 $m\mu$. Therefore, a first order red plate which causes a retardation of 540 $m\mu$ was superimposed on the retardation of the fibers and unravelled material. With this plate in place they were brilliantly colored.

APPENDIX III

DETERMINATION OF INDICES OF REFRACTION BY LINE OF BECKE METHOD

The indices of refraction of the reclassified fibers and the unravelled S_2 layers were measured by the line of Becke method which is carried out as follows:

The fibers (or unravelled S_2 layers) were dried on microscope slides under vacuum at room temperature. The dried fibers were immersed with a Cargille liquid (a nonwetting oil) whose n was known to three decimal places and was close to the expected value. The immersed fibers were viewed between parallel nicols whose plane of vibration was either parallel or perpendicular to the longitudinal fiber axis, depending on which n was being measured. A sodium vapor lamp was used as the illuminant.

Bright yellow lines, the Becke lines, were visible on both edges of the fibers except when the n of the fibers exactly equalled the n of the liquid; in this case, the fibers were invisible. If the Becke lines moved inside the fibers when the microscope tube was raised, it indicated that the n of the fibers was larger than that of the liquid; if the lines moved outside when the tube was raised, the n of the liquid was higher than that of the fibers. With a series of liquids with increasing n 's, the n 's of the fibers were pinned down rapidly.

APPENDIX IV

SUGAR ANALYSES

The chromatographic sugar analysis used in this investigation is Dubey's (53) adaptation of the method of Piper and Bernardin (69). Dubey's technique differs principally in the preparation of the chromatographic paper and in the amounts of spray reagent used.

The acid of the hydrolyzates (see page 41) was neutralized to a pH of six with barium hydroxide. The precipitated barium sulfate was removed by centrifuging, and the neutralized sugars were concentrated to a few milliliters in vacuo. A drop of pyridose solution was added to prevent fermentation and the solutions were stored under refrigeration until used.

The chromatographic separations were made on 9 x 24-in. Whatman no. 1 sheets. The sheets were prewashed with deionized, distilled water for 24 hours in a chromatographic tank, air-dried for one hour, washed for another 24 hours, and air-dried.

The sugars were spotted two inches apart across the top of the sheets. The spots were applied with a microburet within circles whose diameter was less than 5 mm. The spotted sheets were placed into the chromatographic tanks, one to a tray, and allowed to acclimate for 24 hours in an atmosphere at equilibrium with developer in the bottom of the tanks. The developer used was a 9:2:2 mixture of ethyl acetate, acetic acid, and water.

At the end of the acclimatization, 50 ml. of the developer were added to each tray through holes in the covers of the chromatographic tanks. The sheets were left in the tanks until all of the developer had passed to the bottom of the tanks. The developed sheets were air-dried and sprayed uniformly, but very lightly, with a spray reagent to locate the sugars. The reagent contained 0.4 g. *o*-aminobiphenyl in 160 ml. 99.9% glacial acetic acid and 40 ml. of distilled water.

The sheets were oven-dried for exactly five minutes at 105°C. immediately after spraying. The spots (and a blank) were outlined under U.V. light, cut out, weighed, cut into strips, and placed into 150-mm. test tubes. Six milliliters of reagent were added from a buret to each of the test tubes which were then sealed with rubber stoppers covered with aluminum foil. The sugars were eluted by shaking the test tubes vigorously for 25 minutes. The eluates were filtered through glass wool to remove suspended fibers (from the chromatographic paper). The colors of the solutions were developed by heating in a boiling water bath; the pentoses were heated for 30 minutes and the hexoses for 45 minutes. The solutions were cooled rapidly and their absorbances measured against the reagent which had also been heated. The absorbances were measured with a Beckman D.U. spectrophotometer. The amounts of sugar present were determined from concentration-absorbance plots made up from sugar solutions of known concentrations.

APPENDIX V
ORIGINAL DATA

F.P.L. LIGNIN

Sample	Weight of Samples, mg.	Weight of Residues, mg.	F.P.L. Lignin, %
Reclassified fibers	81.13	0.41	0.5
	89.65	.61	.7
	70.08	.36	.5
	142.43	.58	.4
	177.93	.68	.4
			<u>0.5±0.2^a</u>
<u>P-S₁</u> Material	11.50	0.67	5.8
	9.85	.41	4.1
	10.09	.35	3.5
	12.74	.73	5.8
	10.19	.60	5.9
	8.34	.71	8.5
	7.64	.52	6.9
			<u>5.8±3.3</u>
<u>S₂</u> Material	187.06	.76	0.4
	125.34	.52	.4
	171.57	.67	.4
	214.49	.86	.5
	146.12	.66	.4
			<u>0.4±0.1</u>

SUGAR ANALYSES

Sample	Glucose, % ^b	Mannose, % ^b	Xylose, % ^b
Reclassified fibers	89.6	7.1	3.3
	90.8	6.1	3.1
	90.8	6.4	2.8
	<u>90.4±0.6</u>	<u>6.5±0.5</u>	<u>3.1±0.2</u>
<u>P-S₁</u> Material	89.6	6.8	3.6
	91.4	5.6	3.0
	91.7	5.3	3.0
	92.0	4.9	3.1
	<u>91.2±1.0</u>	<u>5.6±0.8</u>	<u>3.2±0.3</u>
<u>S₂</u> Material	86.4	10.2	3.4
	86.4	9.2	4.4
	86.7	9.2	4.1
	86.5	9.8	3.7
	<u>86.5±0.1</u>	<u>9.6±0.5</u>	<u>3.9±0.5</u>

^a 95% confidence limits

^b Per cent of total sugars present

DEGREE OF POLYMERIZATION

Yield of Nitration

Sample	Weight of Sample, mg. ^a	Weight of Nitrated Sample, mg.	Yield, %
Reclassified fibers	16.96	29.06	93.5
P-S ₁ Material	9.85	16.34	90.4
S ₂ Material	18.04	31.26	94.5

^a Corrected for F.P.L. Lignin

Viscosity Measurements

Samples	Flow Time after Dilution with Ethyl Acetate				Intrinsic Viscosity	Average D.P.
	0 ml.	4 ml.	8 ml.	12 ml.		
Reclassified fibers	385.6	274.4	229.1	205.4	27.0	2960
P-S ₁ Material	273.6	216.4	190.8	177.3	18.5	2030
S ₂ Material	396.7	281.3	237.4	208.4	27.5	3050

ALPHA-CELLULOSE AND HEMICELLULOSE DETERMINATIONS

Sample	Weight of Sample, g.	Weight of Alpha-cel- lulose Residue, g.	Per Cent	
			Alpha-cel- lulose, % ^a	Hemi-cel- lulose, % ^a
Reclassified fibers	0.2184	0.1851	84.2	15.3
	.2353	0.1892	83.8	15.7
P-S ₁ Material	0.2208	0.1851	81.3	12.9
S ₂ Material	0.1113	0.0927	82.8	16.8
	.1821	.1511	82.4	17.2

^a Corrected for F.P.L. Lignin